AD-A153 676 COMPARISON OF CALCULATIONS AND MEASUREMENTS OF THE OFF-AXIS RADIATION DOS.. (U) NAVAL POSTGRADUATE SCHOOL MONTEREY CA P F CROMAR DEC 84 1/1

UNCLASSIFIED F/G 9/2 NL

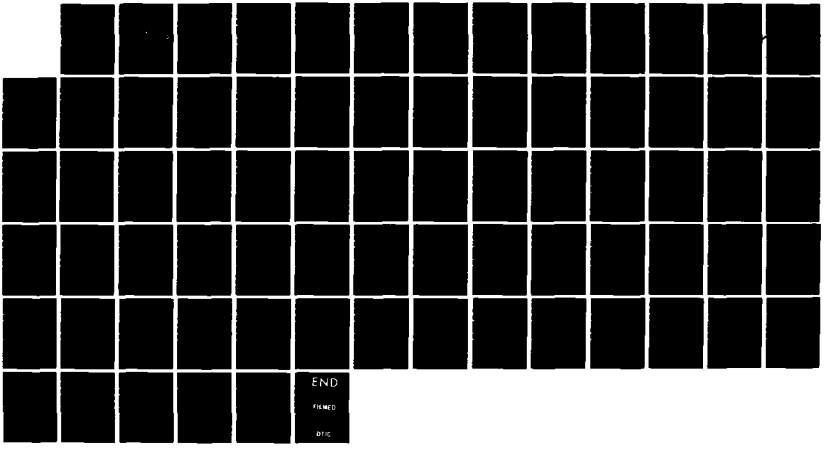

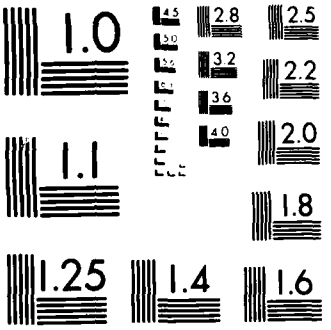

(2)

NAVAL POSTGRADUATE SCHOOL

Monterey, California

THESIS

COMPARISON OF CALCULATIONS AND MEASUREMENTS OF THE OFF-AXIS RADIATION DOSE (SI) IN LIQUID NITROGEN AS A FUNCTION OF RADIATION LENGTH

by

Patrick F. Cromar

December 1984

Thesis Advisor: F. R. Buskirk

SECURITY CLASSIFICATION OF THIS PAGE (When Data Entered)

REPORT DOCUMENTATION PAGE		READ INSTRUCTIONS BEFORE COMPLETING FORM
1. REPORT NUMBER	2. GOVT ACCESSION NO.	3. RECIPIENT'S CATALOG NUMBER
4. TITLE (and Subtitle) Comparison of Calculations and Measurements of the Off-axis Radiation Dose (Si) in Liquid Nitrogen as a Function of Radiation Length		5. TYPE OF REPORT & PERIOD COVERED Master's Thesis December 1984 6. PERFORMING ORG. REPORT NUMBER
7. AUTHOR(s) Patrick F. Cromar		8. CONTRACT OR GRANT NUMBER(s)
9. PERFORMING ORGANIZATION NAME AND ADDRESS Naval Postgraduate School Monterey, California 93943		10. PROGRAM ELEMENT, PROJECT, TASK AREA & WORK UNIT NUMBERS
11. CONTROLLING OFFICE NAME AND ADDRESS Naval Postgraduate School Monterey, California 94943		12. REPORT DATE December 1984 13. NUMBER OF PAGES 72
14. MONITORING AGENCY NAME & ADDRESS(if different from Controlling Office)		15. SECURITY CLASS. (of this report) 15a. DECLASSIFICATION/DOWNGRADING SCHEDULE

16. DISTRIBUTION STATEMENT (of this Report)

Approved for public release; distribution is unlimited

17. DISTRIBUTION STATEMENT (of the abstract entered in Block 20, if different from Report)

18. SUPPLEMENTARY NOTES

19. KEY WORDS (Continue on reverse side if necessary and identify by block number)

Air-Dose, Off-axis Dose, Off-axis Radiation, Bremsstrahlung

20. ABSTRACT (Continue on reverse side if necessary and identify by block number)

Results are presented from the study of the off-axis X and Gamma radiation field caused by a highly relativistic electron beam in liquid Nitrogen at various path lengths out to 2 radiation lengths. The off-axis dose in Silicon was calculated using the electron/photon transport code CYLTRAN and measured using thermal luminescent dosimeters (TLD's). Calculations were performed on a CDC-7600 computer at Los Alamos National Laboratory and measurements were made using the Naval Postgraduate

DD FORM 1 JAN 73 1473 EDITION OF 1 NOV 65 IS OBSOLETE

S/N 0102-LF-014-6601

SECURITY CLASSIFICATION OF THIS PAGE (When Data Entered)

School 100 MeV Linac. Comparision of the results is made and CYLTRAN is found to be in agreement with experimentally measured values. The CYLTRAN results are extended to the off-axis dose caused by a 100 MeV electron beam in air at Standard Temperature and Pressure (STP).

Approved for public release; distribution is unlimited

Comparison of Calculations and Measurements of the Off-axis Radiation Dose (Si) in Liquid Nitrogen as a Function of Radiation Length.

by

Patrick Frank Cromar
Lieutenant, United States Navy
B.S., University of Oregon, 1976

Submitted in partial fulfillment of the requirements for the degree of

MASTER OF SCIENCE IN PHYSICS

from the

NAVAL POSTGRADUATE SCHOOL
December 1984

Author: Patrick F. Cromar
Patrick Frank Cromar

Approved by: Fred R Buskirk
F.R. Buskirk, Thesis Advisor

John R Neighbours
J.R. Neighbours, Second Reader

G E Schacher
Gordon E. Schacher, Chairman
Department of Physics

J. N. Dyer
John N. Dyer,
Dean of Science and Engineering

ABSTRACT

Results are presented from the study of the off-axis X and Gamma radiation field caused by a highly relativistic electron beam in liquid Nitrogen at various path lengths out to 2 radiation lengths. The off-axis dose in Silicon was calculated using the electron/photon transport code CYLTRAN and measured using thermal luminescent dosimeters (TLD's). Calculations were performed on a CDC-7600 computer at Los Alamos National Laboratory and measurements were made using the Naval Postgraduate School 100 Mev Linac. Comparison of the results is made and CYLTRAN is found to be in agreement with experimentally measured values. The CYLTRAN results are extended to the off-axis dose caused by a 100 Mev electron beam in air at Standard Temperature and Pressure (STP).

TABLE OF CONTENTS

LIST OF TABLES

LIST OF FIGURES

I. INTRODUCTION

A. BACKGROUND

When a high energy electron passes through matter it loses energy through two classes of interactions; ionization and bremsstrahlung. At lower energy ionization is the predominant energy loss mechanism while at higher energy bremsstrahlung becomes predominant. Equation 1.1 shows the energy loss by a beam of highly relativistic electrons due to ionization. Equation 1.2 shows the energy loss due to bremsstrahlung for a highly relativistic electron. [Ref. 1]

$$(dE/dx)ion = (4Pie^4\, n/mc^2)\{\log(2mc^2/I) - 3/2(\log(1-B)) - 1/2(\log 8) + 1/16\} \qquad \text{(eqn 1.1)}$$

$$\langle dE/dx\rangle rad = (4NZ^2 r_0^2\, hk/137)\{\log(183/Z^{1/3})\} \qquad \text{(eqn 1.2)}$$

The approximate ratio of energy loss as a function of distance for the two mechanisms is shown in equation 1.3 where E is the electron energy in MeV. Table I contains the meaning of the symbols used in these equations

In the case where the product, EZ is much greater than 800 MeV, energy loss by bremsstrahlung predominates and the energy loss due to ionization may be neglected. The energy at which the ratio is equal to one, for a particular Z, is known as the critical energy and is denoted E(crit). The critical energy in Mev is shown in equation 1.4 . If, in a given material, the incident electron energy is much larger than E(crit) then effectively bremsstrahlung is the only energy loss mechanism until the energy of the electron approaches E(crit). [Ref. 1]

TABLE I

Symbols used in Transport Equations

Symbol	Meaning
Pi	3.14...
n	Electron density
e	Charge on electron
m	Mass of electron
c	Speed of light
I	Ionization potential
B	Ratio of electron velocity to c
h	Planck's constant
N	Atomic density
Z	Atomic number
R	Classical radius of the electron
k	Frequency of the highest energy photon produced

$$(dE/dx)rad/(dE/dx)ion=EZ/800 \qquad \text{(eqn 1.3)}$$

$$E(crit)=800/Z \qquad \text{(eqn 1.4)}$$

Photon production by bremsstrahlung is essentially a statistical process where the energy of any given photon produced in an interaction follows a probability distribution function that is determined by the energy of the electron and the atomic number of the material. The spectrum of energies produced by a mono-energetic electron beam will be very broad, with some photons having a maximum energy equal to that of the incident electron.

The bremsstrahlung produced photons undergo two types of interactions, Compton scattering and Pair Production. At energies above about 10 MeV, pair production dominates the energy loss. The electrons produced in these interactions and the positron produced in pair production undergo further bremsstrahlung. The pair will eventually undergo pair annihilation and produce two low energy gamma rays. This process of bremsstrahlung followed by electron/positron annihilation followed by further bremsstrahlung leads to the formation of what is called a 'radiation shower' [Ref. 2] [Ref. 3]. Figure 1.1 is a graphical representation of shower development.

The work previously cited by Oppenhimer and later work by Rossi was intended for energies greater than the critical energy. This early work was intended to explain the high energy showers detected in the atmosphere as a result of cosmic rays. With the advent of electron accelerators in the hundred MeV and GeV range, their work was applied to the problem of dose buildup in shielding. Since most shielding is made of high Z material the approximation that ionization can be ignored is valid [Ref. 4].

Early work on radiation showers treated energy loss by ionization as just a disappearance of energy from the beam, and did not attempt to treat the electrons formed by the ionization. Since these theories ignore the ionization electrons contribution to the total number of electrons present in the shower, any dose calculation based on these theories would be in error by an amount equal to the contribution of those electrons. For showers formed by extremely energetic electrons the number of ionization formed electrons will remain negligible for a considerable distance [Ref. 3]. In energy regimes where the incident energy is on the order of the critical energy, about 102 MeV for air, the error in a computed dose can be very large.

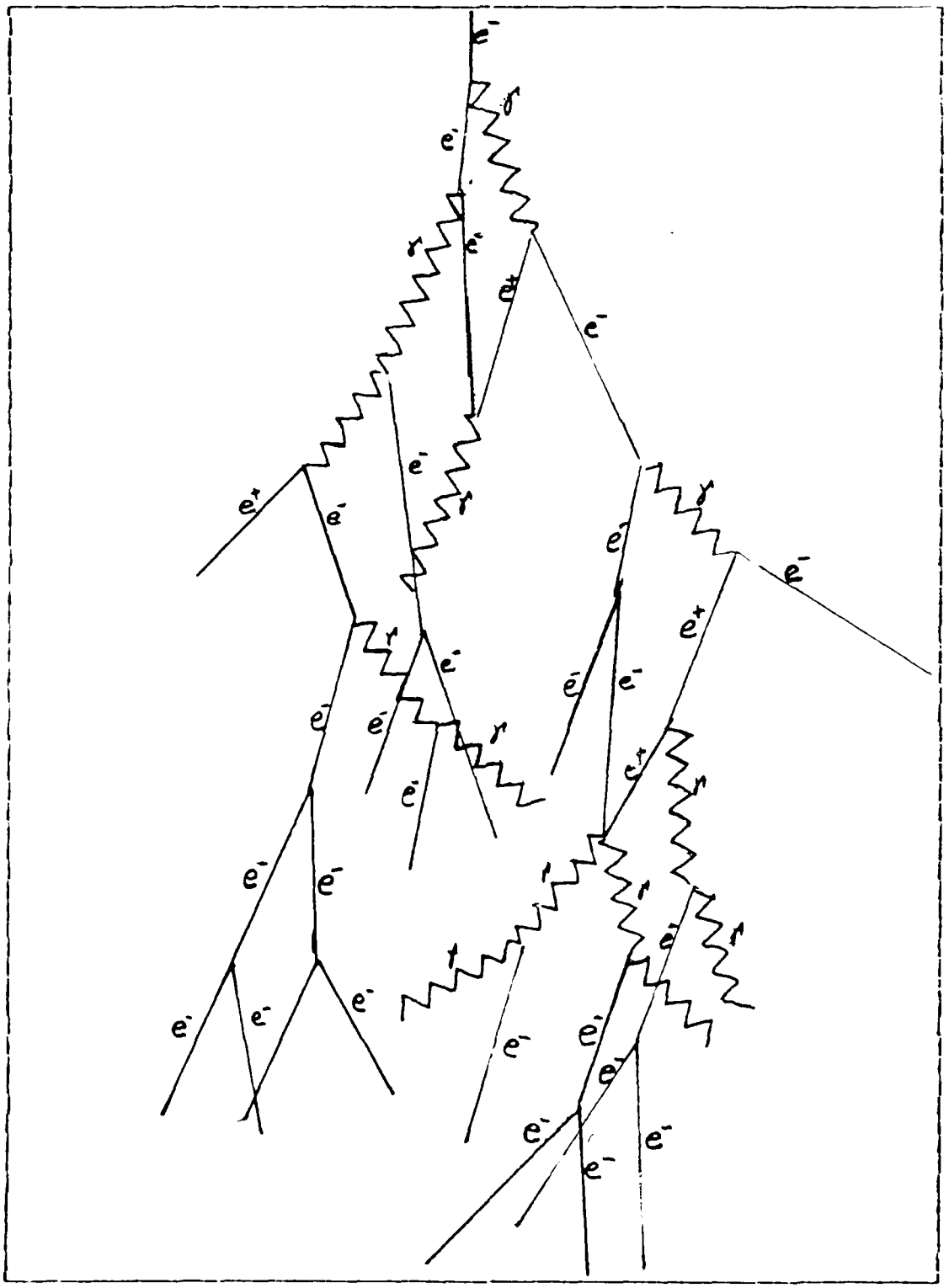

Figure 1.1 Shower Development.

III. EXPERIMENTS

A. DISCUSSION

All experimental runs were conducted at the Naval Postgraduate School using the Electron Linear Accelerator located there. A full description of the NPS Linac is given in [Ref. 7]. Two parameters required close monitoring during experimental runs; the electron energy (all calculations were made for 100 MeV) and the total charge delivered by the accelerator.

The total charge delivered was monitored by a secondary emission monitor (SEM) that was used with a vibrating reed electrometer to determine the total charge delivered to the SEM. Once the total charge to the SEM was known, the total charge delivered was found by using the SEM efficiency factor of 0.06. This represents the largest uncertainty in determining the total charge delivered. Due to uncertainties in the efficiency factor, the total charge delivered can be determined to no better than 5 percent. Electron energy was controlled by the use of a magnetic deflection system whose stability and accuracy is within 0.5%. This is considered to be of sufficient stability and accuracy that any fluctuations would not be noticable within the limits of this set of experiments.

The off-axis dose was measured using Thermal Luminescent Dosimeters (TLD's). TLD's are a class of radiation detectors that utilize an excited electron state to register the deposition of energy. When a TLD is heated the excited electron returns to its ground state and emits a photon. These photons are a direct measure of the amount of energy and hence the dose deposited in the material.

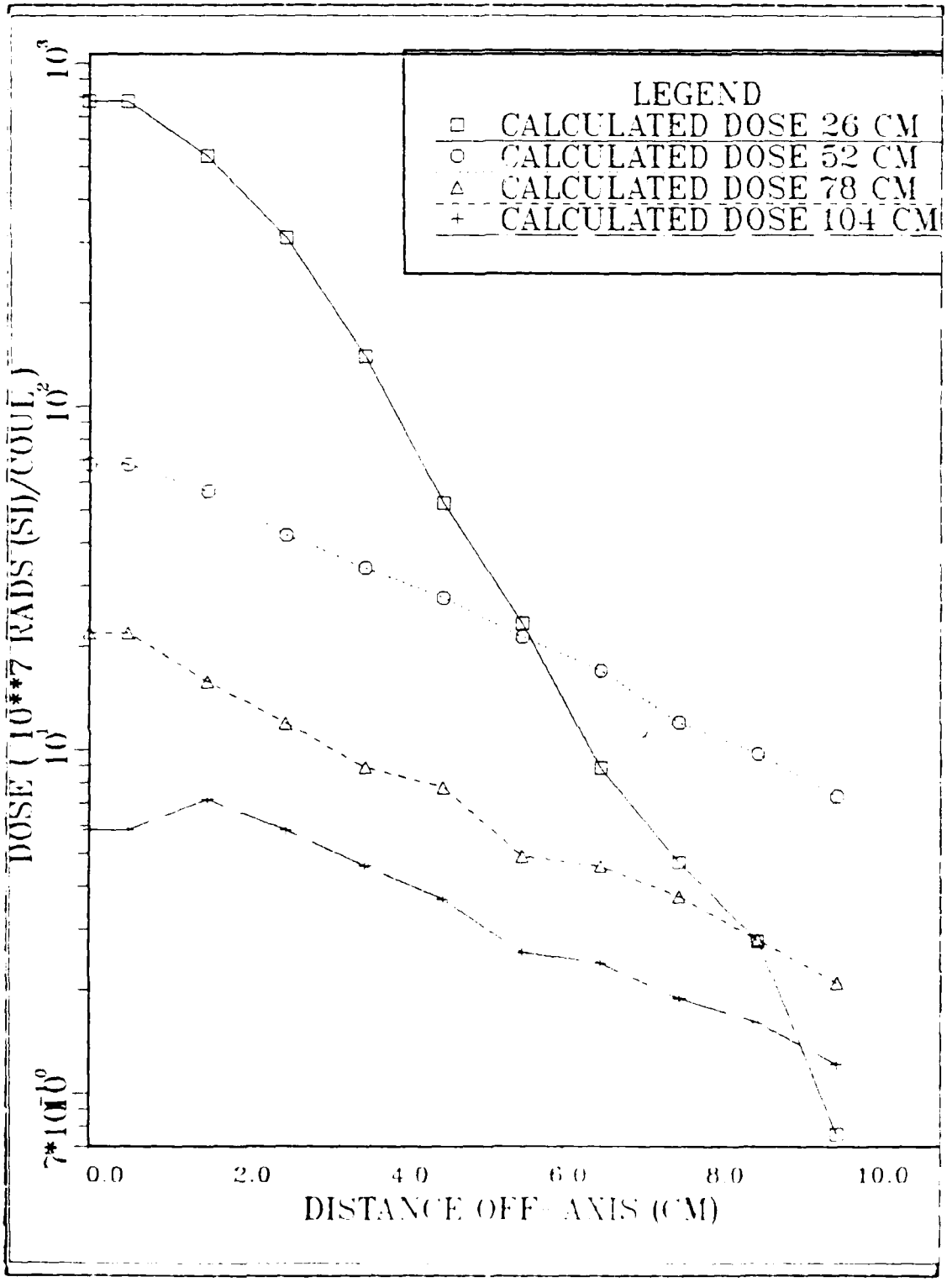

Figure 2.6 Comparison of Off-axis Normalized Doses.

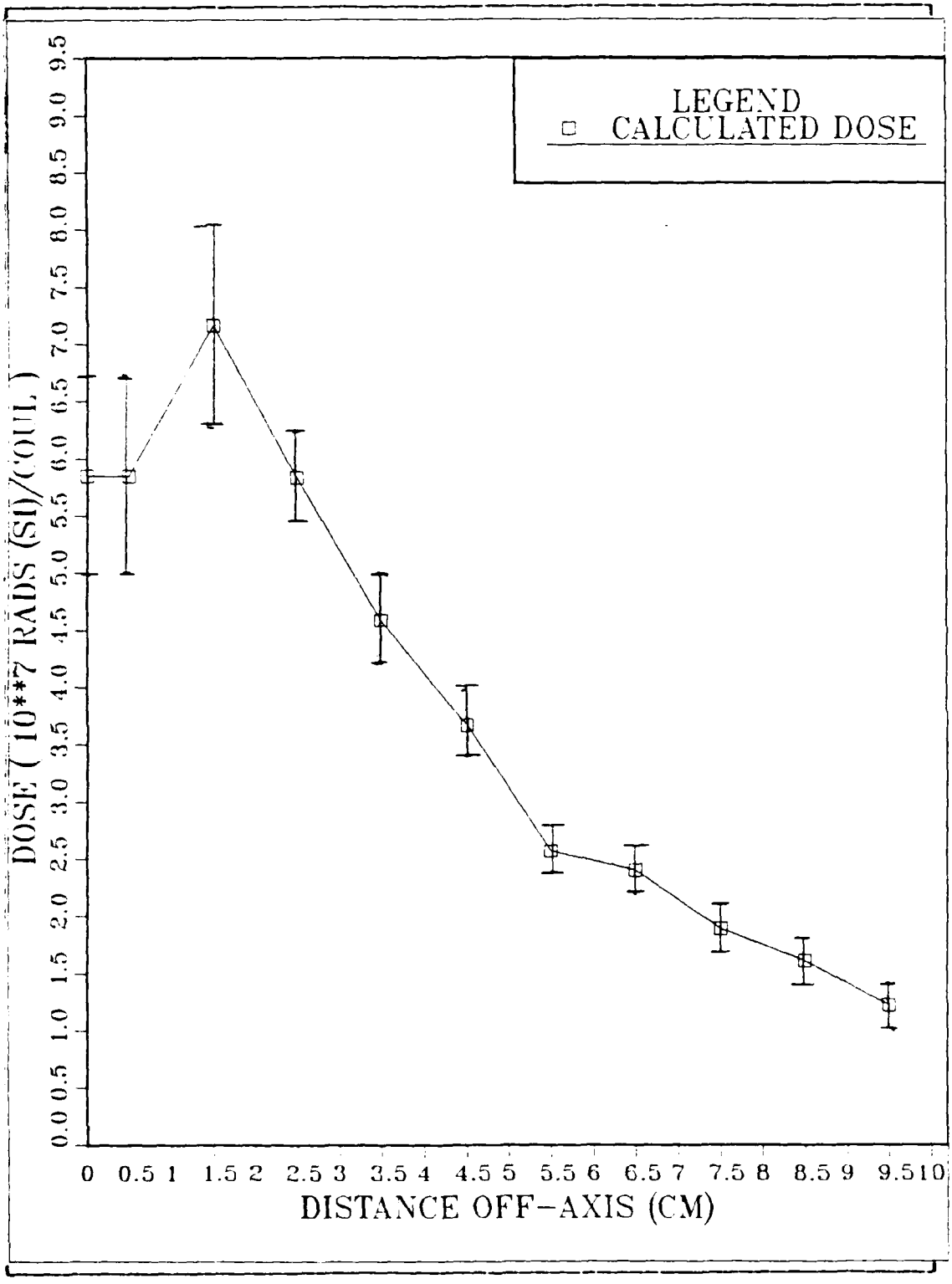

Figure 2.5 Calculated Off-axis Normalized Dose at 104 cm.

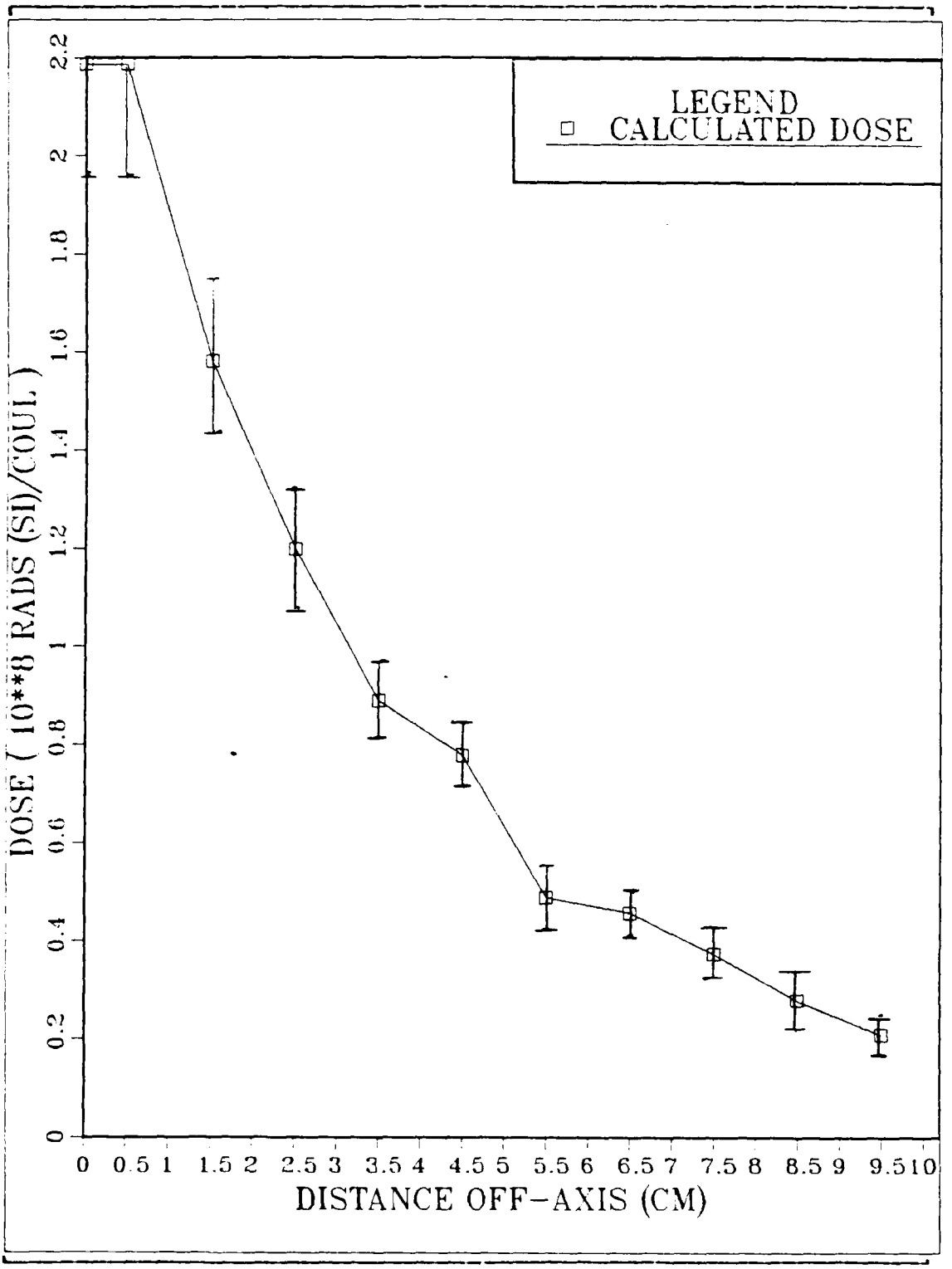

Figure 2.4 Calculated Off-axis Normalized Dose at 78 cm.

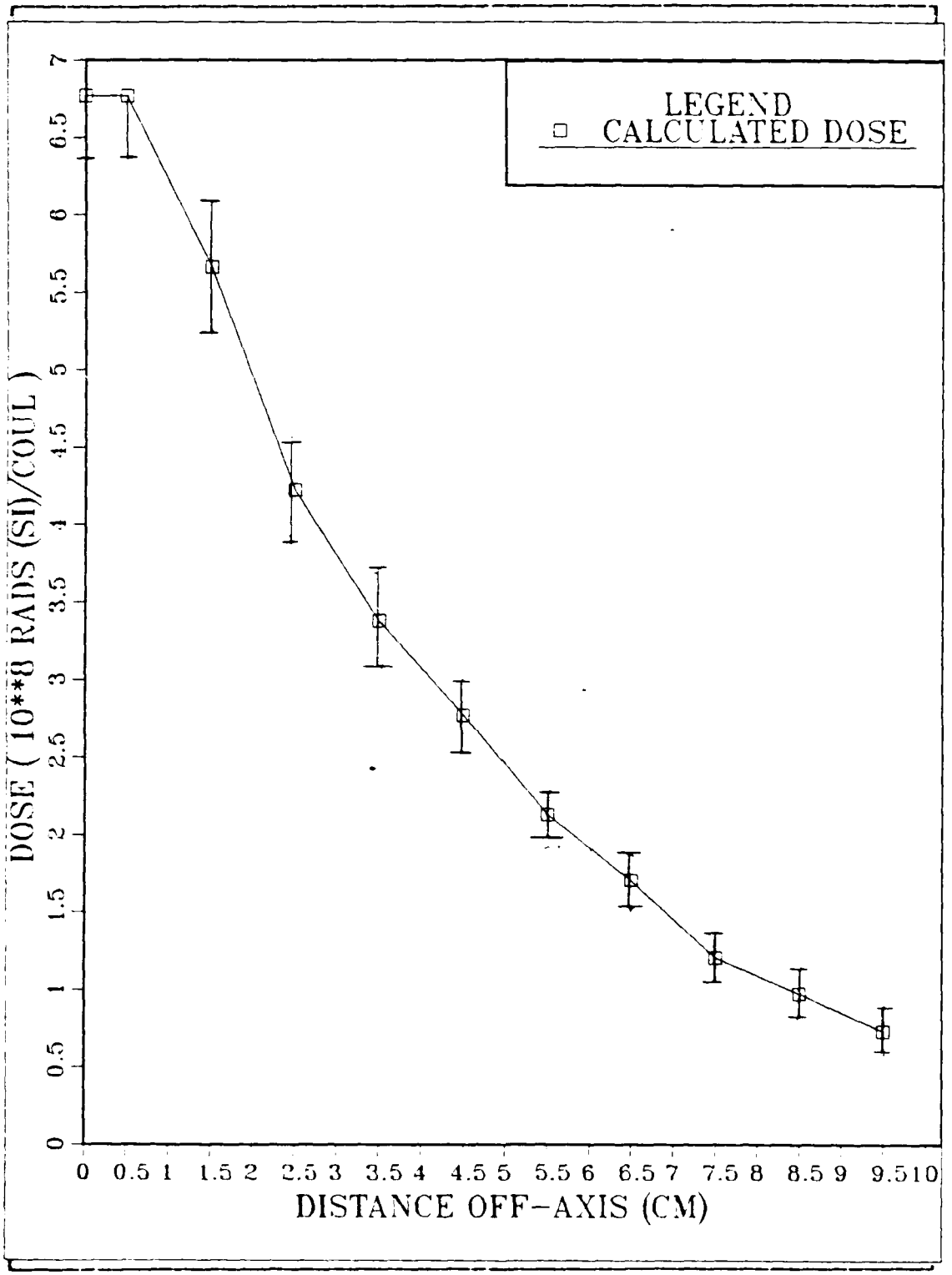

Figure 2.3 Calculated Off-axis Normalized Dose at 52 cm.

CYLTRAN is a relatively large simulation code of about 30,000 lines of fortran. The calculations were performed during an experience tour at the Los Alamos National Laboratories on a CDC-7600 computer. The statistical uncertainties can be seen to grow as the thickness of the liquid Nitrogen is increased. This is due to the exponential rise in the number of interactions that the program must simulate. One method that was used to decrease the statistical uncertainties was to increase the number of incident photons. The drawback to this method is that the number of interactions has already increased exponentially as the length increases, and adding additional incident electrons increases the cpu time of the program even further. It was found that an increase by a factor of two, decreased the statistical uncertainties by only ten percent but increased the cpu time by at least a factor of two. At twenty-six centimeters and with five thousand incident electrons the cpu time was five minutes; at 104 centimeters and with 50,000 incident electrons the cpu time increased to about two hundred minutes.

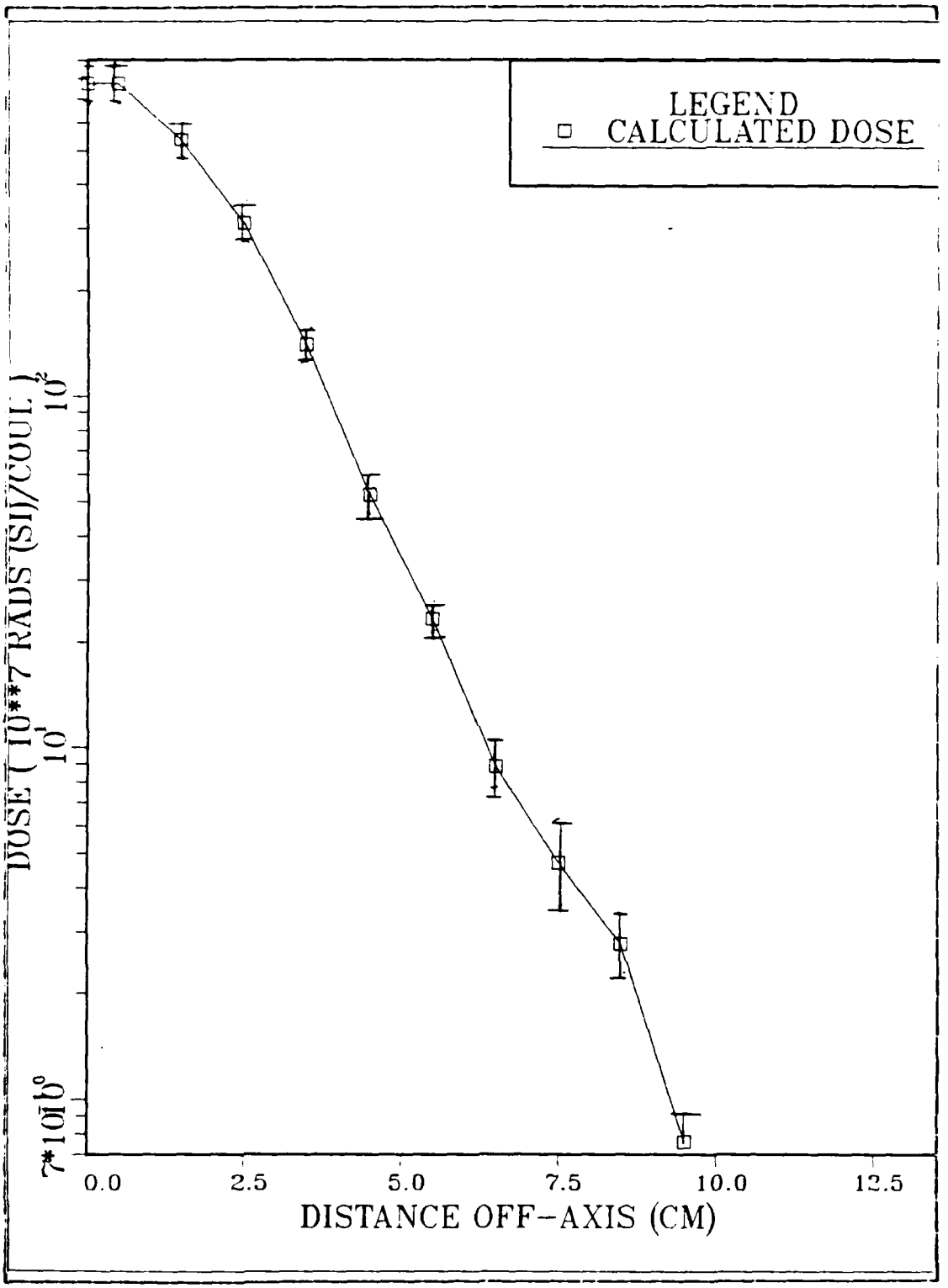

Figure 2.2 Calculated Off-axis Normalized Dose at 26 cm.

TABLE III

Calculated Off-axis Dose

Distance off axis cm	Length of Liquid Nitrogen (normalized dose in Rads (Si) per Coulomb)			
	26 cm.	52 cm.	78 cm.	104 cm.
0.0-1.0	7.773×10^{9} 4	6.771×10^{8} 7	2.187×10^{8} 13	5.847×10^{7} 14
1.0-2.0	5.373×10^{9} 3	5.633×10^{8} 7	1.581×10^{8} 10	7.163×10^{7} 11
2.0-3.0	3.107×10^{9} 2	4.224×10^{8} 7	1.198×10^{8} 10	5.833×10^{7} 6
3.0-4.0	1.402×10^{9} 3	3.380×10^{8} 8	8.879×10^{7} 10	4.583×10^{7} 7
4.0-5.0	5.237×10^{8} 3	2.772×10^{8} 5	7.782×10^{7} 5	3.665×10^{7} 5
5.0-6.0	2.333×10^{8} 5	2.129×10^{8} 4	4.897×10^{7} 7	2.565×10^{7} 3
6.0-7.0	8.855×10^{7} 8	1.704×10^{8} 5	4.579×10^{7} 4	2.397×10^{7} 6
7.0-8.0	4.701×10^{7} 10	1.204×10^{8} 7	3.744×10^{7} 10	1.884×10^{7} 6
8.0-9.0	2.768×10^{7} 16	9.727×10^{7} 5	2.798×10^{7} 12	1.608×10^{7} 6
9.0-10.0	7.588×10^{6} 23	7.329×10^{7} 8	2.095×10^{7} 9	1.215×10^{7} 11

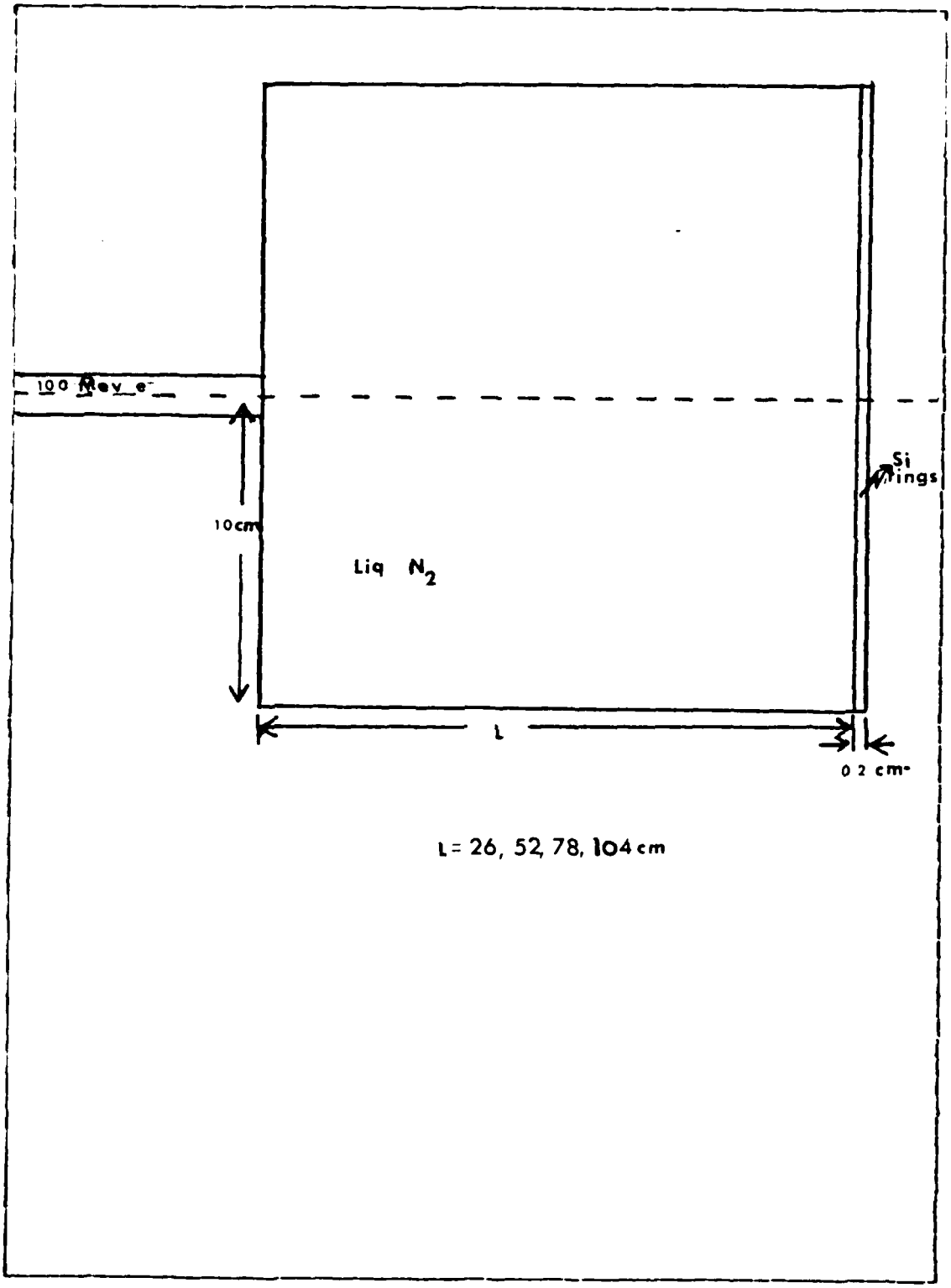

Figure 2.1 CYLTRAN Problem Geometry.

II. CALCULATIONS

A. DESCRIPTION

The cylindrical geometry, multi-material electron/photon Monte-Carlo transport code CYLTRAN was used to calculate the off-axis dose deposited in a 0.2 cm thick silicon target at the desired ranges. The silicon target was divided into ten concentric rings of width 1 centimeter centered on the axis. The simulation geometry is shown in Figure 2.1 . The portion of the CYLTRAN output of interest to this experiment is the energy deposition in each material zone. This portion gives the material, its location and mass, and the energy deposited by primary and knock-on electrons, by photons and the total energy deposited. Each value for the energy deposited includes a one or two digit number that represents the one-sigma statistical uncertainty of the quantity. The deposition data is produced in Mev per incident electron. To simplify future comparisons this data was converted to a normalized dose in units of Rads (Si) per coulomb . Table III contains the total calculated normalized doses, and Figure 2.2 through Figure 2.5 are graphs of the off-axis results. Figure 2.6 is a comparison of the calculated off-axis normalized doses. Appendix A contains the complete CYLTRAN energy deposition data and further information on CYLTRAN.

The assumption that off-axis distances scale linearly with radiation length is based on the work of Oppenhimer and Rossi. Their work shows that the development of a radiation shower is directly related to the position measured in units of the radiation length. The lateral spread of the shower is also dependant on the distance in units of radiation length. For materials with similar Z, it is clear from equation 1.6 that the radiation lengths are in proportion to the ratio of the atomic densities [Ref. 2] [Ref. 3].

TABLE II

Correction of radiation temperature for off-axis distance

centimeters. Since Nitrogen makes up eighty percent of the atmosphere and the next most abundant component, Oxygen differs by an atomic number of one from Nitrogen, the interaction cross section of Nitrogen closely approximates that of the atmosphere. In order to measure the off axis radiation field at several radiation lengths it was decided to substitute liquid Nitrogen for air. Calculations where made using the electron/photon transport code CYLTRAN and are compared to measurements at 26,52,78 and 104 centimeters of liquid nitrogen. The off axis radiation field was calculated and measured at 1 centimeter intervals from on-axis to ten centimeters off- axis. The lengths used in both the calculations and experiments were 26,52,78,104 centimeters of liquid nitrogen corresponding to 0.54, 1.08, 1.63 and 2.17 radiation lengths respectively, Table II compares the experimental lengths to lengths in air including the off-axis distances covered.

In practice, it becomes necessary to use Monte-Carlo techniques to calculate the shower-induced dose. Historically, these codes have been used in a wide variety of problems dealing with shielding and dose buildup [Ref. 5] [Ref. 6]. There appears little published work comparing calculated and measured dose rates in low Z material.

B. DESCRIPTION

It is the purpose of this thesis to determine the off-axis radiation dose deposited in Silicon by a 100 MeV electron beam in liquid Nitrogen, at ranges up to two radiation lengths and extend these result to the off-axis dose in air at STP. This energy is nearly equal to the critical energy which is about 102 MeV [Ref. 4]. The energy of an electron beam is a function of penetration depth and the atomic number of the material. In the case of a mono-energetic electron beam, the beam energy as a function of depth is:

$$\langle E \rangle = E_0 \exp-(x/L) \qquad \text{(eqn 1.5)}$$

where E_0 is the incident energy, x is the depth in the material and L is the radiation length. The radiation length is [Ref. 1] :

$$1/L = (4Z^2 N\hbar_0^2/137)\log(183/Z^{1/3}) \qquad \text{(eqn 1.6)}$$

The radiation length in the standard 80% nitrogen 20% oxygen atmosphere at STP (standard temperature and pressure) is about 307 meters. This poses a significant problem with the Naval Postgraduate School Electron Linear Accelerator (linac) which has an experimental area only two meters in length. The radiation length for liquid Nitrogen is 47.7

Finding a suitable container for the liquid nitrogen posed the first major experimental problem. The TLD's could not be subjected to cryogenic temperatures due to possible mechanical failure. There was also concern that whatever was used to insulate the TLD's might affect the experiment in a undesirable fashion. Due to cost and handling considerations glass dewers were ruled out early in the design phase. Several methods for fabricating a container out of commercially available, closed cell insulation were tried without success. Finally a 1 inch thick, closed cell foam, sheet material was found that could be handled and glued like wood. This material was made into boxes with interior cross sections of 20 X 20 cm and interior lengths of 26, 52, 78 and 104 cm.

The problem of where to position the TLD's was solved by finding the beam axis using a phosphor screen on the TLD side of the container prior to filling with liquid Nitrogen. This allowed positioning of the TLD's to an accuracy of 0.5 cm relative to the beam axis. The TLD's were wrapped in a single layer of 0.3 mil Aluminium and attached to the back of the container with two sided tape. On several runs two lines of TLD's were emplaced, with one set horizontal to the ground and the other vertical; this placement was to determine the extent of any beam asymetries. Table IV list the runs that were made.

TABLE IV

List of Experimental Runs

RUN NUMBER	DATE	LENGTH LIQUID NITROGEN	NUMBER OF TLD's
I	6/27/84	26 cm.	11
II	7/13/84	52 cm.	10
III	7/19/84	26 cm.	14
IV	7/24/84	52 cm.	22
V	7/19/84	78 cm.	22
VI	7/24/84	104 cm.	22

The TLD's were of the Calcium Fluoride type and had been calibrated for use below 30 MeV. Extending the energy observed to 100 Mev may result in low readings; in the event there were gamma rays of high enough energy that the range of the gamma ray produced particle is not negligible compared to the mean free path of the primary particle [Ref. 8]. Clearly this effect will lessen as the length of liquid nitrogen is increased. Unfortunatly, any attempt to correct for this under detection requires a detailed knowledge of the gamma spectrum, which is not available. Since the shortest measurement is at a length greater than 0.5 radiation lengths there will be very few gamma photons with energy greater than 30 MeV and any effect of under detection due to high energy gamma photons should be negligible [Ref. 1].

The TLD's consist of a matrix of teflon holding a low concentration of Calcium Fluoride. Since the absorption cross sections for Calcium Fluoride differ by at most 5 percent from Silicon from 0.1 to 100 MeV the TLD measured dose may be used as dose Silicon [Ref. 9].

B. RESULTS

All TLD's were read at the Naval Surface Weapon Center, White Oak, Maryland. The TLD's were overnight-expressed to NSWC where they were read and the results returned by mail. Results of the experimental runs were reported in Rads, using the charge delivered during the run, these values were converted to Rads per Coulomb. Figure 3.1 through Figure 3.4 show the result of the experimental runs at each length of liquid Nitrogen. Appendix B contains the complete data from the experimental runs.

The vertical error bars in Figures 3.1 through 3.4 are based on the 5 percent non-random uncertainty in determining

the total charge delivered by the Linac and the 5 percent non-random uncertainty resulting from the use of Calcium Fluoride TLD's to measure dose Silicon. This results in a total uncertainty of 10 percent in the measured normalized dose. The horizontal error bars are based on the 0.5 centimeter uncertainty in the position of the TLD's relative to the beam axis.

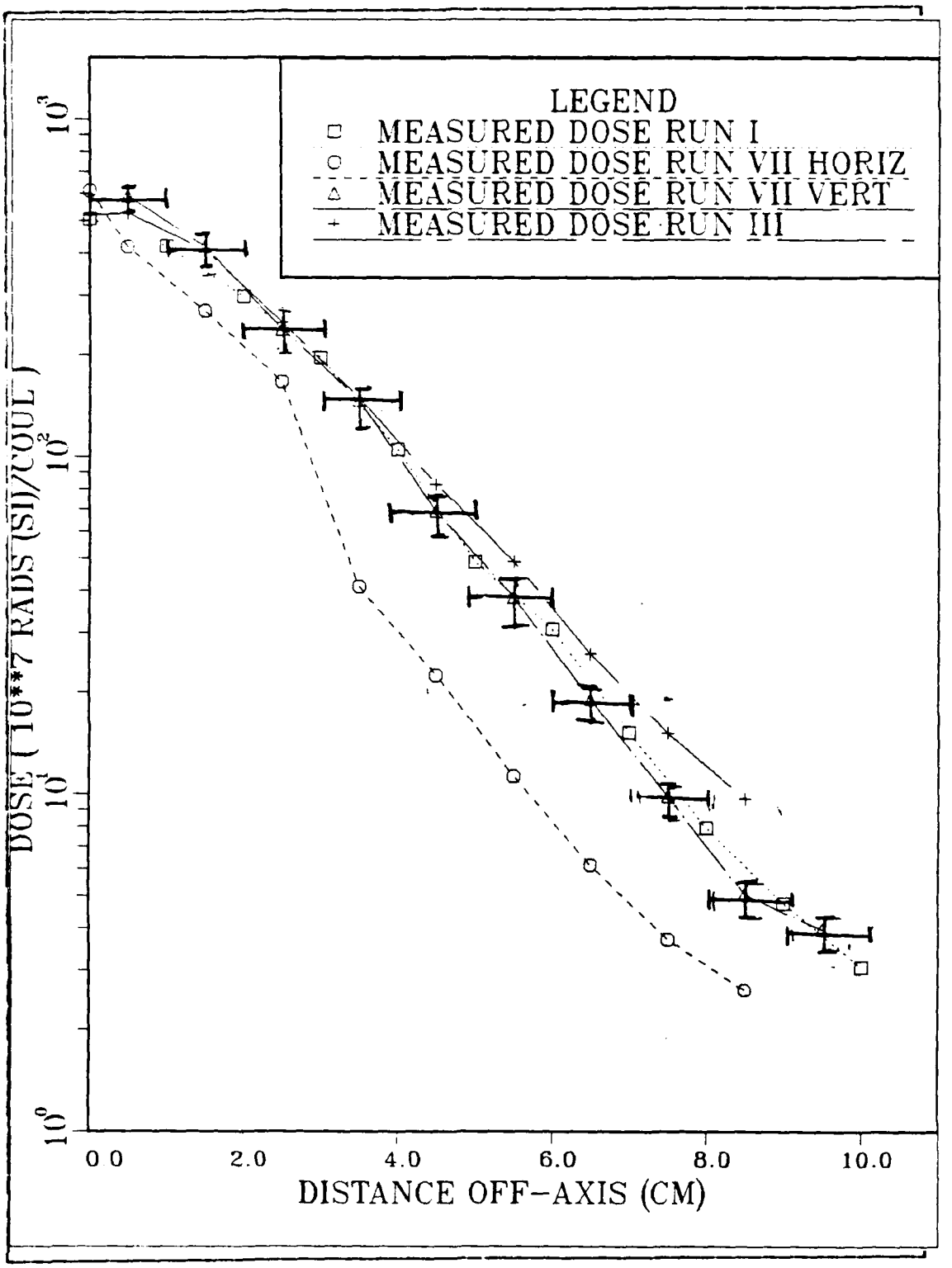

Figure 3.1 Measured Normalized Dose at 26 cm.

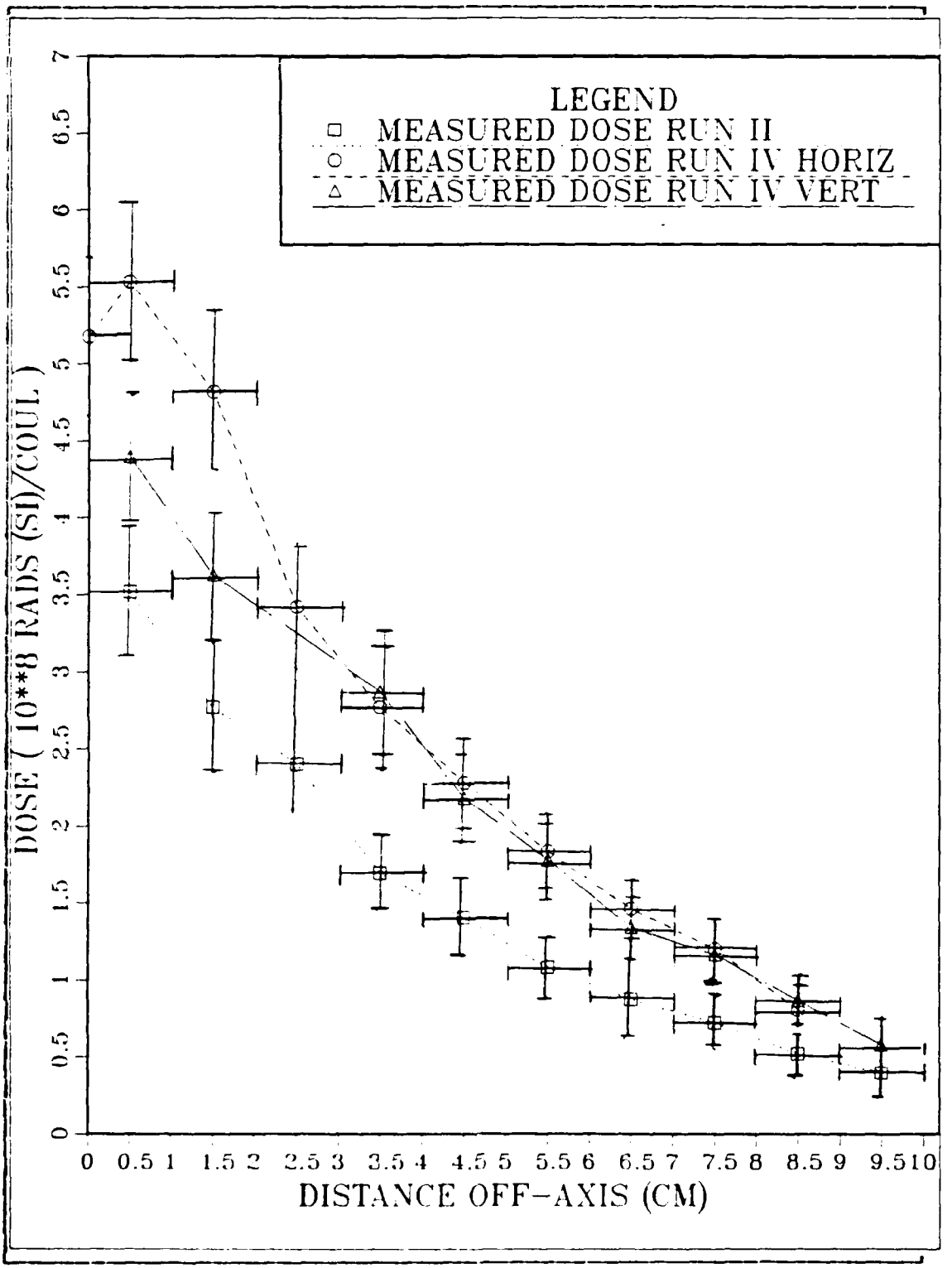

Figure 3.2 Measured Normalized Dose at 52 cm.

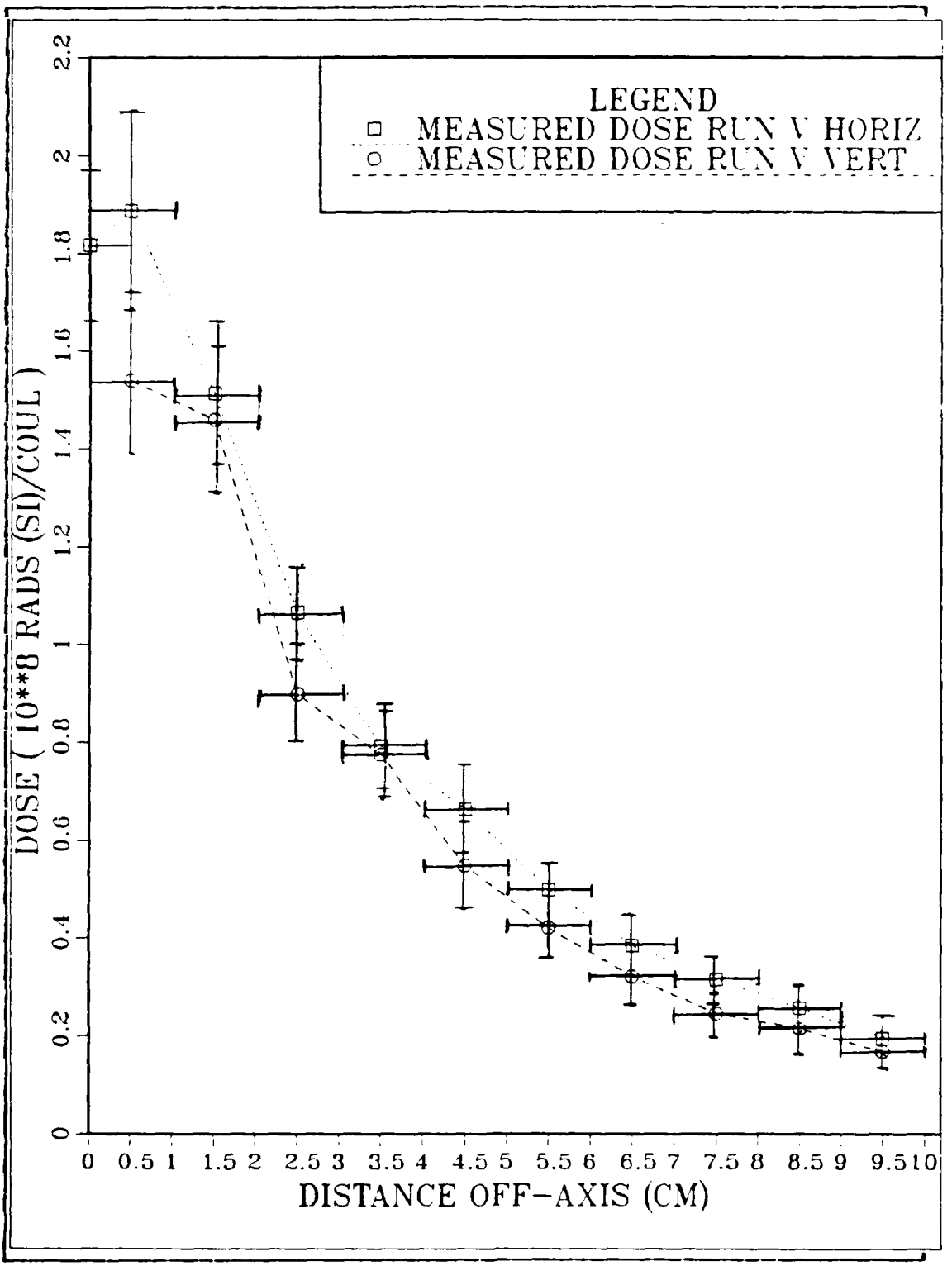

Figure 3.3 Measured Normalized Dose at 78 cm.

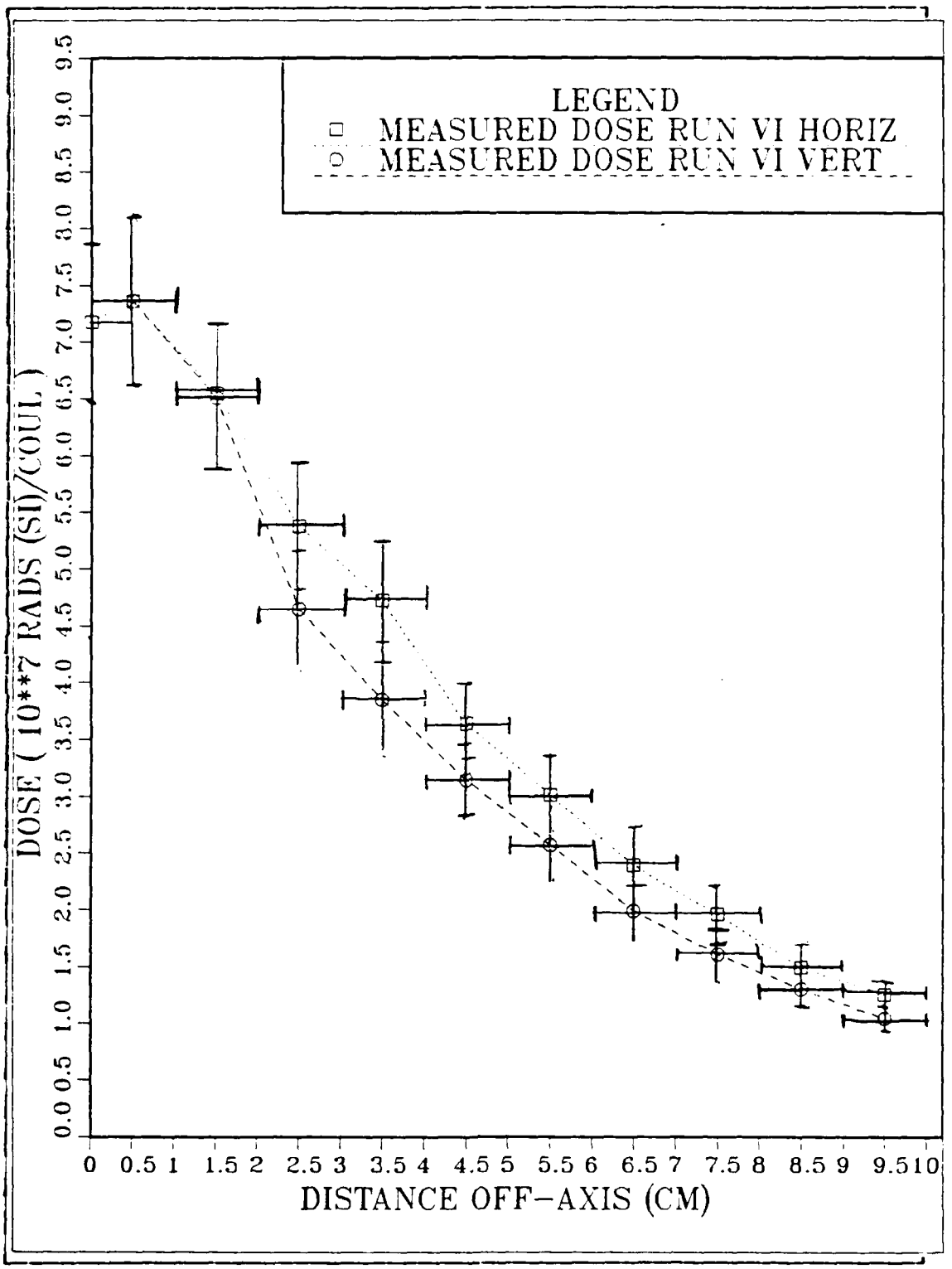

Figure 3.4 Measured Normalized Dose at 104 cm.

IV. CONCLUSIONS

A. DOSE RATE IN LIQUID NITROGEN

Figures 4.1 through 4.4 show the normalized dose as calculated by CYLTRAN and measured with TLD's. The error bars have been left off of the TLD data points in the interest of clarity. Although there is agreement, within a factor of 2 at worst, between measured and the calculated normalized doses, in many cases CYLTRAN appears to calculate higher normalized doses than were measured. The difference between the two normalized doses is not significant and may be due to some undiscovered systematic error.

Measurements at 52, 78, and 104 cm and calculations at 104 cm show a higher normalized dose immediately off-axis than on-axis. This is due to the small solid angle subtended by the on-axis detector; any primary particle that undergoes an interaction will be scatered into a different detector and, since the on-axis detector represent the smallest 'target' of any detector, it will have the lowest probability of having a particle scattered into it.

B. DOSE RATE IN AIR

In order to extend the above results to STP air it is necessary to take into account the change in size, and hence in mass, of the detector as the radiation length increases. The ratio of the radiation lengths in STP air to liquid nitrogen is 647 [Ref. 1]. As mentioned previously, the amount of energy in a shower in some solid angle is a function of the solid angle and the position measured in units of radiation length. If a detector subtends the same solid angle and is located at the same position as measured

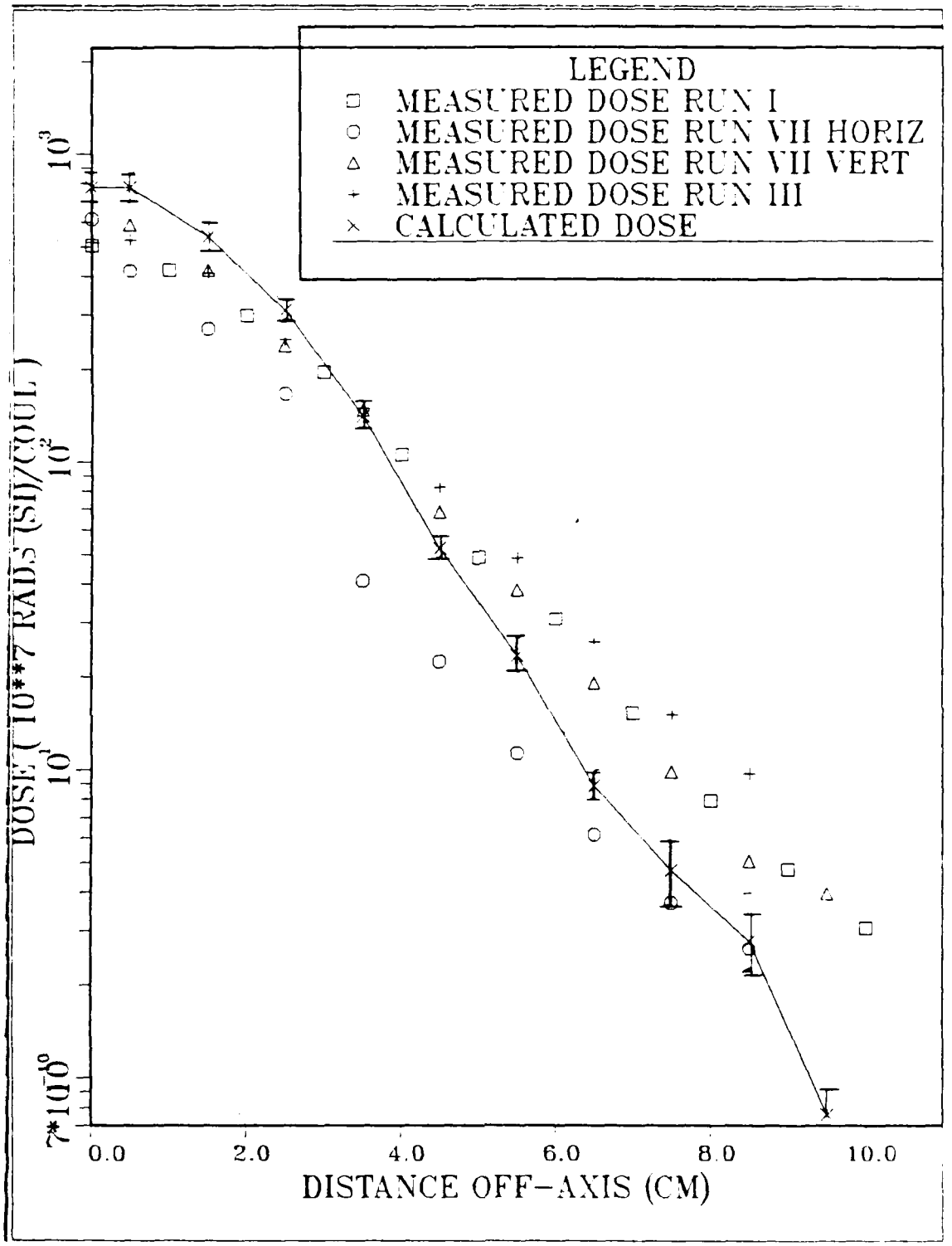

Figure 4.1 Comparison of Experiment and Calculations at 26 cm.

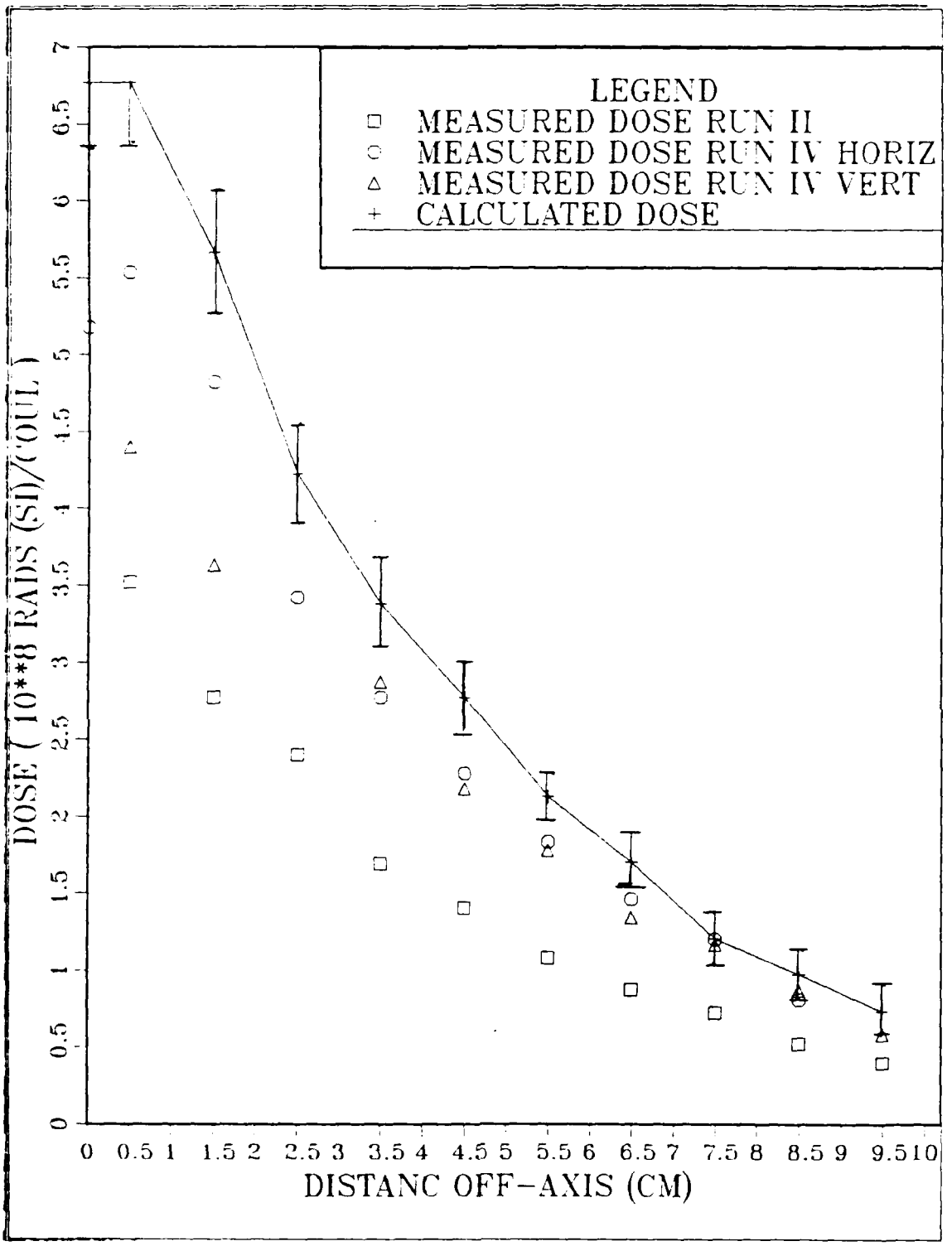

Figure 4.2 Comparison of Experinent and Calculation at 52 cm.

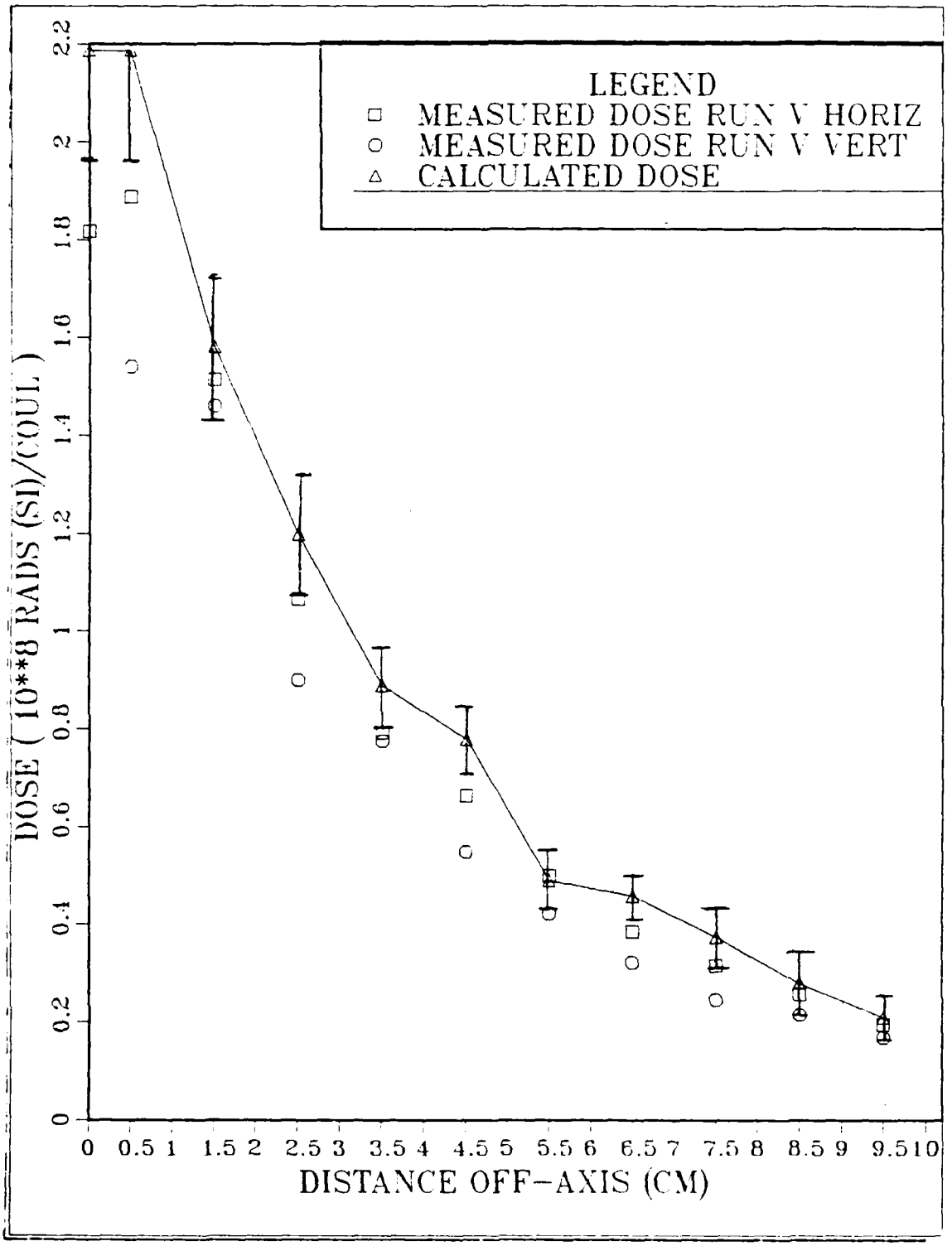

Figure 4.3 Comparison of Experinent and Calculations at 78 cm.

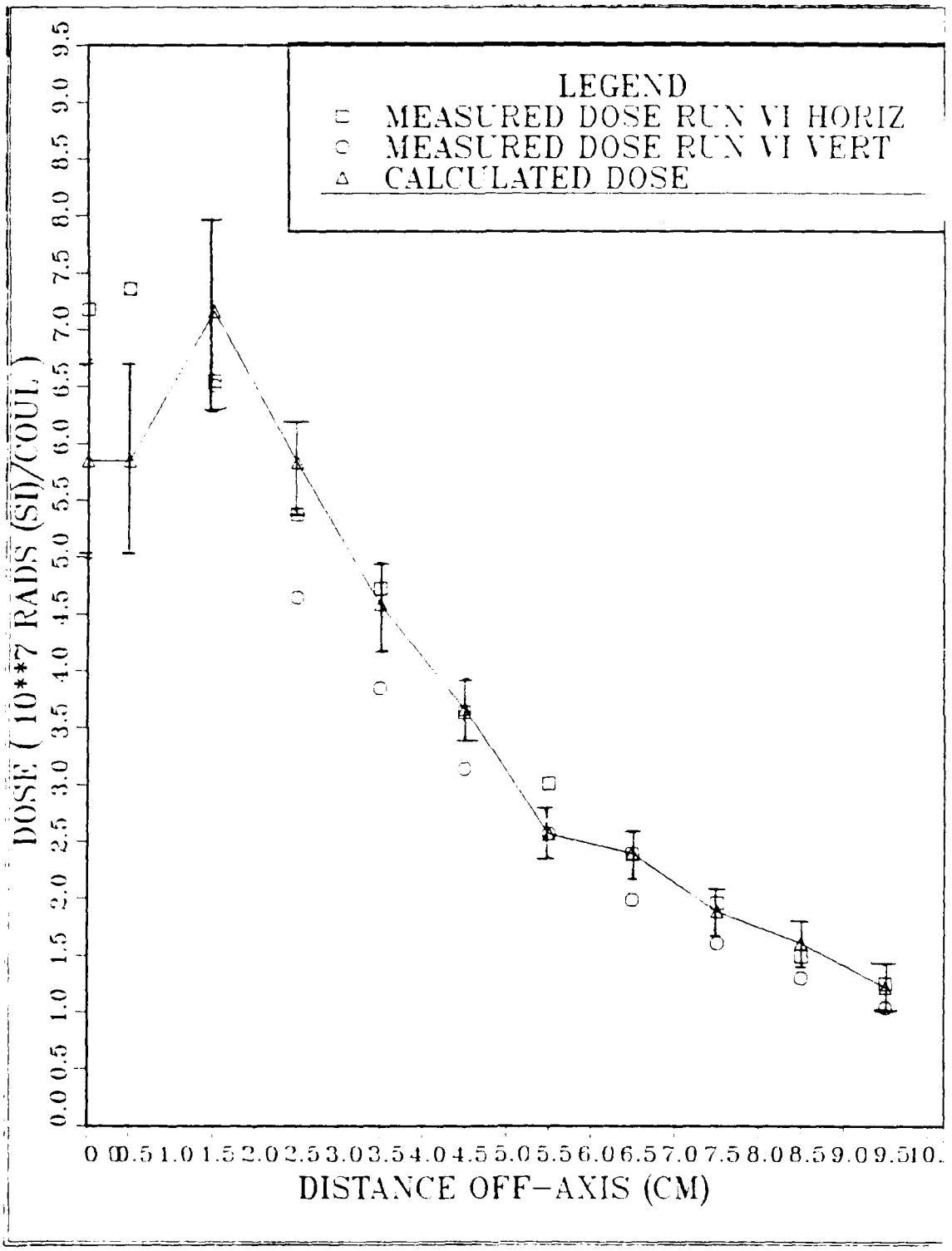

Figure 4.4 Comparison of Experiment and Calculations at 104 cm.

in units of radiation length, then it will absorb the same amount of energy. However the detector will be larger by a factor of the square of the ratio of the radiation lengths; this increase in size will increase the mass and hence decrease the dose. In the case at hand, the dose absorbed by the detector will decrease by 647**2. Table V shows the normalized dose off-axis in STP air for 100 MeV electrons it is based on the CYTRAN calculations in liquid Nitrogen, the distance off- axis is in terms of angle subtended by the detector instead of centimeters.

C. COMPARISON WITH PREVIOUS PAPERS

The only work of a comparable nature found in the open literature is [Ref. 10]. This paper reports the calculated off-axis dose from a 50 MeV electron beam in air at ranges out to 3000 meters. The calculations in [Ref. 10] are based on the computer code ETRAN which was used to calculate the electron and photon distribution emerging from a semi-infinite slab of air. Knowing the photon spectra, the dose in a water sample was calculated. The referenced paper presents the data in Rems per electron with the assumption that 1 Rem equals 1 Rad (H_2O).

Table VI compares selected data points from the tables in [Ref. 10] with the corresponding data points from table V Comparisons in this table are made on the assumption that for that portion of the dose due to Gamma photons 1 Rad(Si) equals 1 Rad (H_2O). No account of the difference in the absorption cross sections for electrons needs to be taken since the referenced report assumes that no electrons directly contribute to the dose. As can be seen in table VI the differences between the normalized doses reported in the referenced paper and the values reported here are significant. At least part of the difference may be attributed to

Table IX

Energy Deposition Data at 26 cm of Liquid Nitrogen (cont'd.)

ZONE	MATERIAL	MASS(grams)	VOLUME(cc)
1	1	6.61619E+03	8.16813E+03
2	2	1.46398E+00	6.28318E-01
3	2	4.39194E+00	1.88495E+00
4	2	7.31990E+00	3.14159E+00
5	2	1.02479E+01	4.39823E+00
6	2	1.31758E+01	5.65485E+00
7	2	1.61038E+01	6.91150E+00
8	2	1.90318E+01	8.16813E+00
9	2	2.19597E+01	9.42477E+00
10	2	2.48877E+01	1.06814E+01
11	2	2.78156E+01	1.19380E+01

TABLE IX

Energy Deposition Data at 26 cm of Liquid Nitrogen

ENERGY DEPOSITION
(normalized to one incident particle)

	****ENERGY DEPOSITED (MeV)****			
ZONE	PRIMARIES	KNOCK-ONS	GAMMA-SEC	TOTAL
1	3.78260E+01 00	-6.51166E-01 03	3.36420E+00 02	4.05390E+01 00
2	8.62524E-02 02	4.19244E-03 85	2.33159E-02 05	1.13797E-01 04
3	1.85092E-01 02	4.15902E-03 99	4.67363E-02 03	2.35988E-01 03
4	1.88997E-01 01	8.51412E-04 99	3.76066E-02 04	2.27455E-01 02
5	1.26838E-01 02	-3.23919E-03 99	2.00851E-02 07	1.43684E-01 03
6	6.13308E-02 04	-1.79455E-03 78	9.46974E-03 10	6.90060E-02 03
7	3.29772E-02 04	-7.59269E-05 99	4.67150E-03 13	3.75728E-02 05
8	1.27884E-02 11	8.75726E-04 91	3.18869E-03 19	1.68529E-02 08
9	7.90177E-03 11	-2.18102E-06 99	2.42386E-03 17	1.03234E-02 10
10	5.56047E-03 20	1.08246E-04 99	1.13026E-03 13	6.88898E-03 16
11	1.90698E-03 27	-4.47756E-04 99	6.51317E-04 19	2.11054E-03 23

Table VIII

Input File for 104 cm Liquid Nitrogen Calculation (cont'd.)

```
FILE 3:
     1     6     6     5     5 50000    11
          0.0         104.0          0.0          10.0    1
        104.0         104.2          0.0           1.0    2
        104.0         104.2          1.0           2.0    2
        104.0         104.2          2.0           3.0    2
        104.0         104.2          3.0           4.0    2
        104.0         104.2          4.0           5.0    2
        104.0         104.2          5.0           6.0    2
        104.0         104.2          6.0           7.0    2
        104.0         104.2          7.0           8.0    2
        104.0         104.2          8.0           9.0    2
        104.0         104.2          9.0          10.0    2
        100.0           0.5          0.2           1.0          1.0
     1    10           10
          20.0         10.0          7.0           4.0          1.0          0.5
          20.0         10.0          7.0           4.0          1.0          0.2
          20.0         40.0         60.0          80.0        180.0        180.0
          20.0         40.0         60.0          80.0        180.0        180.0
```

TABLE VIII

Input Files for 104 cm. Liquid Nitrogen Calculation

FILE 1:

```
     2      1
    1
    7       1.0
    1
   14       1.0
```

FILE 2:

```
** Input file for 104 cm liquin Nitrogen run
    1        100.0         0.81
    1        100.0         2.33
```

Table VII

CYLTRAN Input Variable and Formats (cont'd.)

NZ	Blank
NR	Blank
TIN	Equals EMAX.
TCUT	Cutoff energy at which electron histories are terminated.
TPCUT	Cutoff energy at which photon histories are terminated.
CTHIN	Cosine of the divergence of the particle source equals 1.0 for non-divergent beam.
SORCIN	Radius of source at left planner boundary.

Table VII

CYLTRAN Input Variable and Formats (cont'd.)

INC	1 for incident electrons, 2 for incident photons.
JMAX	Number of energy bins for classifying escaping electrons and energy. absorption in the target.
JPMAX	Number of energy bins for classifying escaping photons and energy absorption in the target.
KMAX	Number of angular bins used to classify escaping electrons.
KPMAX	Number of angular bins used to classify escaping photons.
IMAX	Total number of primary particles
NZON	Number of zones for which a input line (#7) is required.
NB	Number of batches to be run; if blank or 0 set to 10.
ZLI	Z coordinate of left boundary of zone in cm.
ZRI	Z coordinate of right boundary of zone in cm.
RII	Radius of inner cylindrical boundary of zone in cm.
ROI	Radius of outer cylindrical boundary of zone in cm.
MATI	Material index of the zone as determined by the order in which line #2 and 3 are read; 0 is used for voids.
IZR	Subzoning (left blank).

VII

CYLTRAN Input Variables and Formats (cont'd.)

* The Lines #2,3,5 must be repeated NMAT times; the order #2,3 must be the same as that of the repeated #5.

** Line #7 must be repeated NZON times.

*** Continue on additional cards if necessary.

Variables are defined below:

NMAT	Number of unique materials used in problem (=<5).
NSET	Arbitrary set number
NE	Number of in the target material (=<10).
IZ	Array of Atomic numbers of the constituent elements in ascending ord
W	Weight fraction corresponding to IZ array (follows IZ array).
Comment	A 72 character comment describing the run
ISTATE	1 for a solid or liquid, 2 for a gas.
EMAX	Incident electron energy.
RHO	NTP ($0^{o}c$, 1 atm) density of the target (gm/cm^{3})
ETA	Ratio of actual density to the NTP Density in the target. If blank set to 1.0.

TABLE VII

CYLTRAN Input Variables and Formats

Line No.	Variable	Formats
File 1:		
1	NMAT,NSET	(12I6)
2*	NE	(I5)
3*	(IZ(J), W(J), J=1,NE)	(5(I5, E10.0))***
File 2:		
4	COMMENT	18A4
5*	ISTATE, EMAX, RHO, ETA	(I5, 3F12.5)
file 3:		
6	INC, JMAX, KMAX, KPMAX, IMAX, NZON, NB	(12I6)
7**	ZLI, ZRI, RIT, ROI, MATI, IZR, NZ, NR	(4E12.5, 4I4)
8	TIN, TCUT, TPCUT, CTHIN, SORCIN	(6F12.5)
9	LDSAV, NRING, RADMAX	(2I6, F12.5)
10	JMAX ELECTRON ENERGY BINS	(50F12.5)
11	JPMAX PHOTON ENERGY BINS	(50F12.5)
12	KMAX ELECTRON ANGULAR BINS	(36F12.5)
13	KPMAX PHOTON ANGULAR BINS	(36F12.5)

CYLTRAN combines condensed history electron Monte Carlo calculations with conventional single scattering Monte Carlo methods. [Ref. 5] [Ref. 11]. The code follows electron transport including energy-loss straggling, elastic scattering and the production of knock-on electrons, bremsstrahlung, characteristic X-rays and annihilation radiation. Photon transport includes the coverage of photoelectric, Compton and pair production interactions and includes secondary particle production.

The cross sections for electron interactions are obtained from the ETRAN Monte Carlo system [Ref. 12] while the photon cross sections are calculated from analytical fits of Biggs and Lighthill [Ref. 13]. Although the problem geometry is limited to two dimensions all particle geometries are generated and followed in three dimensions.

The geometry used to generate the data used here is shown in figure 2.1 . The problem geometry is rather simple, consisting of a cylinder of liquid nitrogen ten centimeters in radius and varying in length for the different runs. The Silicon end is set at 0.2 centimeters in thickness and is divided into ten concentric rings each of which is one centimeter in width. Beam divergence was left at zero.

Only three input files were required to run each problem [Ref. 11] table VII shows the input parameters, their format and their meaning. The problem inputs were varied as to the number of energy bins and angular bins in order to minimize the statistical uncertainties. Table VIII is a listing of the input tables used in calculating the off-axis dose at 104 cm. The values shown for the energy bins and the energy cutoff values were used for all calculations. Final energy deposition outputs for the four problem geometries are shown in table IX , table X , table XI and table XII

APPENDIX A
DESCRIPTION OF CYLTRAN AND OUTPUT

The computer code CYLTRAN which was used for the calculations of the off-axis dose rates in this thesis is a cylindrical-geometry multimaterial electron/photon transport code. The code was developed at Sandia National Laboratories by J.A. Halbleib and W.H. Vandevender [Ref. 11]. The code is written in Fortran IV and was run on a CDC-7600 at Los Alamos National Laboratories.

CYLTRAN describes the generation and the transport of the electron/photon shower from the incident energy down to a cut-off energy of 1.0 and 10.0 Kev for electrons and photons, respectively. The user may specify a higher cut-off energy for either or both the electrons and photons. The materials (up to ten) that the shower propagates through must be invariant with respect to rotations about some axis. The incident particles may be either electrons or photons, they may be mono-energetic or have a source spectrum specified. The incident particles may also be either; mono-directional (no divergence), have a divergence angle specified or be isotropic. The output of cyltran contains the following main categories of data:

a) Charge and energy distribution profiles.

b) Integral energy and number escape coefficients for both electrons and photons.

c) Escape coefficients for electrons and photons that are differential in energy, angle and in both energy and angle.

TABLE VI

Comparison of Reported Results

Distance in air (meters)	Angular displacement (degrees)	CYLTRAN Rads/Coul	Reference Rads/Coul
330	5.5-10	220	20
500	0.0-0.5	520	60
670	0.0-0.5	140	30

All values for distance and normalized dose were rounded off to the nearest decade.

Table V

Off-Axis Normalized Doses in STP Air (cont'd.)

	504.8 m
0.0-0.7	$5.20X10^{2}$
0.7-1.5	$3.77X10^{2}$
1.5-2.2	$2.86X10^{2}$
2.2-2.9	$2.12X10^{2}$
2.9-3.7	$1.85Z10^{2}$
3.7-4.4	$1.16X10^{2}$
4.4-5.1	$1.09X10^{2}$
5.1-5.8	$8.9X10^{1}$
5.8-6.6	$6.6X10^{1}$
6.6-7.3	$5.0X10^{1}$
	673.1 m
0.0-0.5	$1.39X10^{2}$
0.5-1.1	$1.71X10^{2}$
1.1-1.6	$1.39X10^{2}$
1.6-2.2	$1.09X10^{2}$
2.2-2.7	$8.7X10^{1}$
2.7-3.3	$6.1X10^{1}$
3.3-3.8	$5.7X10^{1}$
3.8-4.4	$4.5X10^{1}$
4.4-4.9	$3.8X10^{1}$
4.9-5.5	$2.9X10^{1}$

TABLE V

Off-Axis Normalized Doses in STP Air

Angular displacement (degrees)	Length of STP air (normalized dose in Rads per coulomb (Si))
	168.2 m
0.0-2.2	1.856×10^{4}
2.2-4.4	1.283×10^{4}
4.4-6.6	7.418×10^{3}
6.6-8.7	3.347×10^{3}
8.7-10.9	1.250×10^{3}
10.9-13.0	5.57×10^{2}
13.0-15.1	2.11×10^{2}
15.1-17.1	1.12×10^{2}
17.1-19.1	6.6×10^{1}
19.1-21.0	1.8×10^{1}
	336.5 m
0.0-1.1	1.617×10^{3}
1.1-2.2	1.345×10^{3}
2.2-3.3	1.008×10^{3}
3.3-4.4	8.07×10^{2}
4.4-5.5	6.61×10^{2}
5.5-6.6	5.08×10^{2}
6.6-7.7	4.06×10^{2}
7.7-8.7	2.87×10^{2}
8.7-9.8	2.32×10^{2}
9.8-10.9	1.75×10^{2}

tne difference in incident energy; additionally the assumption made in [Ref. 10] that the primary, knock-on and the photon produced (secondary) electrons do not directly contribute to the dose will cause an under-calculation of the dose. The detailed analysis necessary to determine the exact source of the differences is beyond the scope of this thesis.

TABLE X

Energy Deposition Data at 52 cm of Liquid Nitrogen

ENERGY DEPOSITION
(normalized to one incident particle)

	****ENERGY DEPOSITED (MeV)****			
ZONE	PRIMARIES	KNOCK-ONS	GAMMA-SEC	TOTAL
1	5.99592E+01 00	-3.01048E-01 03	1.03467E+01 01	7.00049E+01 00
2	2.40926E-03 16	7.12945E-04 52	6.78983E-03 10	9.91204E-03 07
3	7.77432E-31 09	-1.54086E-04 99	1.72522E-02 07	2.48724E-02 07
4	1.26765E-02 07	-3.79346E-04 99	1.86243E-02 09	3.09215E-02 07
5	1.62144E-02 06	-8.66416E-04 99	1.92901E-02 08	3.46380E-02 08
6	1.94424E-02 08	-3.44083E-03 25	2.05225E-02 08	3.65241E-02 05
7	1.94827E-02 05	1.27008E-04 99	1.46814E-02 07	3.42911E-02 04
8	2.00288E-02 08	6.33822E-05 99	1.23304E-02 04	3.24226E-02 05
9	1.65246E-02 09	-2.90002E-04 99	1.01972E-02 07	2.64318E-02 07
10	1.58962E-02 08	-1.42149E-04 99	8.45353E-03 11	2.42076E-02 05
11	1.21177E-02 10	3.05019E-04 72	7.86941E-03 12	2.03852E-02 08

Table X

Energy Deposition Data at 52 cm of Liquid Nitrogen (cont'd.)

ZONE	MATERIAL	MASS(grams)	VOLUME(cc)
1	1	6.61619E+03	8.16813E+03
2	2	1.46398E+00	6.28318E-01
3	2	4.39194E+00	1.88495E+00
4	2	7.31990E+00	3.14159E+00
5	2	1.02479E+01	4.39823E+00
6	2	1.31758E+01	5.65485E+00
7	2	1.61038E+01	6.91150E+00
8	2	1.90318E+01	8.16813E+00
9	2	2.19597E+01	9.42477E+00
10	2	2.48877E+01	1.06814E+01
11	2	2.78156E+01	1.19380E+01

TABLE XI

Energy Deposition Data at 78 cm of Liquid Nitrogen

ENERGY DEPOSITION
(normalized to one incident particle)

	****ENERGY DEPOSITED (MeV)****			
ZONE	PRIMARIES	KNOCK-ONS	GAMMA-SEC	TOTAL
1	1.11192E+01 00	-3.16719E-01 03	1.52905E+01 01	7.60930E+01 00
2	0.0 E+00 00	-2.03708E-04 99	3.40613E-03 11	3.20242E-03 13
3	0.0 E+00 99	1.87147E-04 99	6.75465E-03 09	6.94179E-03 10
4	0.0 E+00 99	2.19759E-04 99	8.54669E-03 09	8.76645E-03 10
5	0.0 E+00 99	1.04735E-04 99	8.[illegible]432E-03 09	9.09905E-03 10
6	0.0 E+00 99	9.02742E-06 99	1.02444E-02 04	1.02534E-02 05
7	0.0 E+00 99	4.35256E-04 38	7.45032E-03 07	7.88558E-03 07
8	0.0 E+00 99	5.41172E-05 99	8.66136E-03 03	8.71548E-03 04
9	0.0 E+00 99	-2.18329E-05 99	8.20012E-03 10	8.22196E-03 10
10	0.0 E+00 99	1.85088E-04 50	6.77836E-03 12	6.96345E-03 12
11	0.0 E+00 99	1.78158E-04 45	5.64985E-03 09	5.82801E-03 09

Table XI

Energy Deposition Data at 78 cm of Liquid Nitrogen (cont'd)

ZONE	MATERIAL	MASS(grams)	VOLUME(cc)
1	1	6.61619E+03	8.16813E+03
2	2	1.46398E+00	6.28318E-01
3	2	4.39194E+00	1.88495E+00
4	2	7.31990E+00	3.14159E+00
5	2	1.02479E+01	4.39823E+00
6	2	1.31758E+01	5.65485E+00
7	2	1.61038E+01	6.91150E+00
8	2	1.90318E+01	8.16813E+00
9	2	2.19597E+01	9.42477E+00
10	2	2.48877E+01	1.06814E+01
11	2	2.78156E+01	1.19380E+01

TABLE XII

Energy Deposition Data at 104 cm of Liquid Nitrogen

ENERGY DEPOSITION
(normalized to one incident particle)

	****ENERGY DEPOSITED (MeV)****			
ZONE	PRIMARIES	KNOCK-ONS	GAMMA-SEC	TOTAL
1	6.13884E+01 00	-3.08836E-01 03	1.74117E+01 01	7.84993E+01 00
2	0.0 E+00 99	4.13909E-05 99	1.75519E-03 22	1.79658E-03 21
3	0.0 E+00 99	-4.38325E-04 61	3.22420E-03 17	2.78587E-03 18
4	0.0 E+00 99	-3.41882E-05 99	3.86302E-03 08	3.82883E-03 09
5	0.0 E+00 99	-1.48069E-04 94	4.31434E-03 12	4.16627E-03 11
6	0.0 E+00 99	2.21297E-05 99	4.55413E-03 09	4.57626E-03 09
7	0.0 E+00 99	2.32657E-04 71	5.78241E-03 09	6.01506E-03 08
8	0.0 E+00 99	2.82965E-04 49	4.23207E-03 07	4.51504E-03 09
9	0.0 E+00 99	2.04372E-04 51	4.13296E-03 12	4.33733E-03 12
10	0.0 E+00 99	1.61622E-04 43	3.70618E-03 06	3.86781E-03 07
11	0.0 E+00 99	-2.35826E-04 99	3.18591E-03 13	2.95008E-03 17

Table XII

Energy Deposition Data at 104 cm of Liquid Nitrogen (cont'd.)

ZONE	MATERIAL	MASS(grams)	VOLUME(cc)
1	1	6.61619E+03	8.16813E+03
2	2	1.46398E+00	6.28318E-01
3	2	4.39194E+00	1.88495E+00
4	2	7.31990E+00	3.14159E+00
5	2	1.02479E+01	4.39823E+00
6	2	1.31758E+01	5.65485E+00
7	2	1.61038E+01	6.91150E+00
8	2	1.90318E+01	8.16813E+00
9	2	2.19597E+01	9.42477E+00
10	2	2.48877E+01	1.06814E+01
11	2	2.78156E+01	1.19380E+01

APPENDIX B
EXPERIMENTAL RESULTS

The tables in this appendix contain the results of the six experimental runs. Uncertainty in charge delivered is 5 percent, uncertainty in the normalized dose is 10 percent and uncertainty in off-axis position is 0.5 cm.

TABLE XIII

Experimental Run I

Length of Liquid Nitrogen: 26 cm.
Charge Delivered to SEM: 1.0 E-06 coul.
Total Charge Delivered: 1.5 E-05 coul.

TLD POSITION (off-axis)	DOSE MEASURED (Rads)	NORMALIZED DOSE (Rads per Coul)
0.0 cm.	8.43 E+04	5.05 E+09
1.0	7.00 E+04	4.20 E+09
2.0	4.96 E+04	2.97 E+09
3.0	3.26 E+04	1.95 E+09
4.0	1.75 E+04	1.00 E+09
5.0	8.12 E+03	4.87 E+08
6.0	5.13 E+03	3.07 E+08
7.0	2.54 E+03	1.52 E+08
8.0	1.32 E+03	7.92 E+07
9.0	0.70 E+03	4.74 E+07
10.0	0.51 E+03	3.06 E+07

TABLE XIV

Experimental Run JI

Length of Liquid Nitrogen: 52 cm.
Charge Delivered to SEM: 4.4 E-06 coul.
Total Charge Delivered: 7.33 E-05 coul.

TLD POSITION (off-axis)	DOSE MEASURED (Rads)	NORMALIZED DOSE (Rads per Coul)
0.5 cm.	2.58 E+04	3.51 E+08
1.5	4.41 E+04	2.76 E+08
2.5	1.76 E+04	2.40 E+08
3.5	1.24 E+04	1.69 E+08
4.5	1.03 E+04	1.40 E+08
5.5	7.9 E+03	1.07 E+08
6.5	6.39 E+03	8.71 E+07
7.5	5.29 E+03	7.21 E+07
8.5	3.83 E+03	5.22 E+07
9.5	2.85 E+03	3.88 E+07

TABLE XV

Experimental Run III

Length of Liquid Nitrogen: 26 cm.
Charge Delivered tc SEM: 1.00 E-06 coul.
Total Charge Delivered: 1.67 E-05 coul.

TLD POSITION (off-axis)	DOSE MEASURED (Rads)	NORMALIZED DOSE (Rads per Coul)
0.0 cm.	8.62 E+04	5.17 E+09
0.5	8.76 E+04	5.25 E+09
1.5	6.83 E+04	4.09 E+09
2.5	4.14 E+04	2.48 E+09
3.5	2.48 E+04	1.47 E+09
4.5	1.38 E+04	8.27 E+08
5.5	8.10 E+03	4.85 E+08
6.5	4.40 E+03	2.64 E+08
7.5	2.52 E+03	1.51 E+08
8.5	1.62 E+03	9.69 E+07
9.5	1.04 E+03	6.24 E+07
10.0	0.52 E+03	3.13 E+07

TABLE XVI

Experimental Run IV

Length of Liquid Nitrogen: 52 cm.
Charge Delivered to SEM: 8.8 E-06 coul.
Total Charge Delivered: 1.35 E-04 coul.

TLD POSITION (off-axis)	DOSE MEASURED (Rads)	NORMALIZED DOSE (Rads per Coul)
(horizontal)		
0.0 cm.	6.99 E+04	5.17 E+08
0.5	7.47 E+04	5.53 E+08
1.5	6.51 E+04	4.82 E+08
2.5	4.62 E+04	3.42 E+08
3.5	3.74 E+04	2.77 E+08
4.5	3.08 E+04	2.28 E+08
5.5	2.47 E+04	1.83 E+08
6.5	1.97 E+04	1.46 E+08
7.5	1.62 E+04	1.20 E+08
8.5	1.09 E+04	8.07 E+07
9.5	failed	

Table XVI
Experimental Run IV (cont'd.)

TLD POSITION (off-axis)	DOSE MEASURED (Rads)	NORMALIZED DOSE (Rads per Coul)
(vertical)		
0.5	5.94 E+04	4.40 E+08
1.5	4.90 E+04	3.62 E+08
2.5	failed	
3.5	3.79 E+04	2.80 E+08
4.5	2.94 E+04	2.17 E+08
5.5	2.40 E+04	1.77 E+08
6.5	1.81 E+04	1.34 E+08
7.5	1.57 E+04	1.16 E+07
8.5	1.17 E+04	8.67 E+07
9.5	7.85 E+03	5.81 E+07
10.5	6.93 E+03	5.13 E+07

TABLE XVII

Experimental Run V

Length of Liquid Nitrogen: 78 cm.

Charge Delivered to SEM: 2.8 E-05 coul.

Total Charge Delivered: 4.75 E-04 coul.

TID POSITION (off-axis)	DOSE MEASURED (Rads)	NORMALIZED DOSE (Rads per Coul)
(horizontal)		
0.0 cm.	8.63 E+04	1.81 E+08
0.5	8.97 E+04	1.88 E+08
1.5	7.19 E+04	1.51 E+08
2.5	5.06 E+04	1.06 E+08
3.5	3.76 E+04	7.92 E+07
4.5	3.15 E+04	6.63 E+07
5.5	2.37 E+04	4.99 E+07
6.5	1.83 E+04	3.85 E+07
7.5	1.50 E+04	3.16 E+07
8.5	1.22 E+04	2.57 E+07
9.5	9.31 E+03	1.96 E+07
10.0	9.63 E+03	2.03 E+07

table XVII

Experimental Run V (cont'd.)

TID POSITION (off-axis)	DOSE MEASURED (Rads)	NORMALIZED DOSE (Rads per Coul)
(vertical)		
0.5	7.33 E+04	1.54 E+08
1.5	6.95 E+04	1.46 E+08
2.5	4.27 E+04	8.99 E+07
3.5	3.68 E+04	7.75 E+07
4.5	2.60 E+04	5.47 E+07
5.5	2.00 E+04	4.21 E+07
6.5	1.53 E+04	3.22 E+07
7.5	1.17 E+04	2.46 E+07
8.5	1.02 E+04	2.15 E+07
9.5	8.03 E+03	1.69 E+07

TABLE XVIII

Experimental Run VI

Length of Liquid Nitrogen: 104 cm.
Charge Delivered tc SEM: 5.0 E-05 coul.
Total Charge Delivered: 8.33 E-04 coul.

TLD POSITION (off-axis)	DOSE MEASURED (Rads)	NORMALIZED DOSE (Rads per Coul)
(horizontal)		
0.0 cm.	5.98 E+04	7.18 E+07
0.5	6.13 E+04	7.36 E+07
1.5	5.46 E+04	6.55 E+07
2.5	4.48 E+04	5.38 E+07
3.5	3.93 E+04	4.72 E+07
4.5	3.03 E+04	3.64 E+07
5.5	2.51 E+04	3.01 E+07
6.5	1.99 E+04	2.39 E+07
7.5	1.63 E+04	1.96 E+07
8.5	1.24 E+04	1.49 E+07
9.5	1.04 E+04	1.25 E+07
10.0	9.55 E+03	1.15 E+07

Table XVIII

Experimental Run VI (cont'd.)

TLD POSITION (off-axis)	DOSE MEASURED (Rads)	NORMALIZED DOSE (Rads per Coul)
(vertical)		
0.5	6.13 E+04	7.36 E+07
1.5	5.42 E+04	6.51 E+07
2.5	3.87 E+04	4.65 E+07
3.5	3.21 E+04	3.85 E+07
4.5	2.62 E+04	3.14 E+07
5.5	2.14 E+04	2.57 E+07
6.5	1.66 E+04	1.99 E+07
7.5	1.34 E+04	1.61 E+07
8.5	1.08 E+04	1.30 E+07
9.5	8.70 E+03	1.04 E+07

LIST OF REFERENCES

1. Segre, E., Nuclei and Particles, W.A. Benjaman, Reading Massachusetts, 1977

2. Oppenheimer, J. R. and Carlson, J. F., "On Multiplicative Showers," Physical Review, v. 51, pp. 220-265, 15 February 1937

3. Rossi, B. B., High Energy Particles, Prentice-Hall, New York, 1952

4. Swanson, W.P., Radiological Safety Aspects of the Operation of Electron Linear Accelerators, International Atomic Energy Agency, Vienna, 1979

5. Berger, M.J., Methods in Computational Physics Vol I, pp. 135-217, Academic Press, 1963

6. Berger, M. J. and Seltzer, S.M., "Bremsstrahlung and Photoneutrons from Thick Tungsten and Tantalum Targets" Physical Review, v. 2c (2), 1970

7. Barnett, M.T. and Cunneen, W.J., Design and Performance of the Electron Linear Accelerator at the U.S. Naval Postgraduate School, M.S. Thesis, Naval Postgraduate School, Monterey, California, 1966

8. Attix F.H. and Roesch W.C., Radiation Dosimetry, Academic Press, New York, 1966

9. National Bureau of Standard Report 82-2550-A Stopping Power and Ranges of Electrons and Positrons, by M.J. Berger, and S.M. Seltzer, 1982

10. Naval Research Laboratory Report 3335 Calculated Photon Spectra and Radiation Dose From 50 MeV Electrons Stopping in Air, by R.A. Lindgren, 1976

11. Sandia National Laboratories Report SAND 74-0030 CYLTRAN: A Cylindrical-Geometry Multimaterial Electron/Photon Transport Code, by J.A. Halbleib Sr., and W.H. Vandevender, 1964

12. Berger, M.J. and Seltzer, S.M., ETRAN Monte Carlo Code System for Electron and Photon Transport Through Extended Media, Radiation Shielding Information Center, Computer Code Collection, Oak Ridge National Laboratory, 1968

13. Sandia National Laboratories Report SC-RR-68-619 Analytical Approximations for Total Pair-Production Cross Sections, by F. Biggs, and R. Lighthill, 1967

INITIAL DISTRIBUTION LIST

		No. Copies
1.	Defence Technical Information Center Cameron Station Alexandria, Virgina 22314	2
2.	Library, Code 0142 Naval Postgraduate School Monterey, California 93943	2
3.	Professor F. R. Buskirk, Code 61Bs Naval Postgraduate School Monterey, California 93943	5
4.	Professor J. R. Neighbours, Code 61Nb Naval Postgraduate School Monterey, California 93943	2
5.	Professor K. Woehler, Code 61Wh Naval Postgraduate School Monterey, California 93943	2
6.	Dr. R. A. Lindgren Department of Physics University of Massachussets Amherst, Massachussets 01033	1
7.	Dr. J. A. Hableib Sandia Laboratories Theoretical Division 5223 Albuqurgue, New Mexico 87115	2
8.	A. Smith Naval Surface Weapons Center Code H-23 White Oak, Maryland 20810	5
9.	Dr. M. W. Cromar National Bureau of Standards Boulder, Colorado 80303	1
10.	P. F. Cromar Stategic Systems Project Office Code 27301 Crystal City, Virgina 20362	3
11.	Xavier Maruyama, Code 61Xa Naval Postgraduate School Monterey, California 93943	2

END

FILMED

6-85

DTIC